

Machine learning for detection of stenoses and aneurysms: application in a physiologically realistic virtual patient database

Gareth Jones¹, Jim Parr², Perumal Nithiarasu¹, and Sanjay Pant^{1, †}

¹*College of Engineering, Swansea University, Swansea, United Kingdom.*

²*McLaren Technology Centre, Woking, United Kingdom.*

[†]*Corresponding author: Sanjay.Pant@swansea.ac.uk*

Abstract

This study presents an application of machine learning (ML) methods for detecting the presence of stenoses and aneurysms in the human arterial system. Four major forms of arterial disease—carotid artery stenosis (CAS), subclavian artery stenosis (SAC), peripheral arterial disease (PAD), and abdominal aortic aneurysms (AAA)—are considered. The ML methods are trained and tested on a physiologically realistic virtual patient database (VPD) containing 28,868 healthy subjects, which is adapted from the authors previous work and augmented to include the four disease forms. Six ML methods—Naive Bayes, Logistic Regression, Support Vector Machine, Multi-layer Perceptron, Random Forests, and Gradient Boosting—are compared with respect to classification accuracies and it is found that the tree-based methods of Random Forest and Gradient Boosting outperform other approaches. The performance of ML methods is quantified through the F_1 score and computation of sensitivities and specificities. When using all the six measurements, it is found that maximum F_1 scores larger than 0.9 are achieved for CAS and PAD, larger than 0.85 for SAS, and larger than 0.98 for both low- and high-severity AAAs. Corresponding sensitivities and specificities are larger than 90% for CAS and PAD, larger than 85% for SAS, and larger than 98% for both low- and high-severity AAAs. When reducing the number of measurements, it is found that the performance is degraded by less than 5% when three measurements are used, and less than 10% when only two measurements are used for classification. For AAA, it is shown that F_1 scores larger than 0.85 and corresponding sensitivities and specificities larger than 85% are achievable when using only a single measurement. The results are encouraging to pursue AAA monitoring and screening through wearable devices which can reliably measure pressure or flow-rates.

Keywords— virtual patients, stenosis, aneurysm, pulse wave haemodynamics, screening, machine learning

1 Introduction

Two of the most common forms of arterial disease are stenosis, narrowing of an arterial vessel, and aneurysm, an increase in the area of a vessel. They are estimated to affect between 1% and 20% of the population [1–4], and ruptured abdominal aortic aneurysms alone are estimated to cause 6,000–8,000 deaths per year in the United Kingdom [5]. Current methods for the detection of arterial disease are primarily based on direct imaging of the vessels, which can be expensive and hence prohibitive for large-scale screening. If arterial disease can be detected by easily acquirable pressure and flow-rate measurements at select locations within the arterial network, then large-scale screening may be facilitated.

It is likely that the indicative biomarkers of arterial disease in the pressure and flow-rate profiles consist of micro inter- and intra-measurement details. In the past, detection of arterial disease has been proposed through the analysis of waveforms in combination with mathematical models of pulse wave propagation, see for example [6, 7]. This, however, requires specification or identification of patient-specific network parameters, which is not easy to perform, especially at large scales.

This study explores the use of Machine Learning (ML) methods for the detection of stenoses and aneurysms in order to facilitate large scale low-cost screening/diagnosis. A data-driven ML approach is adopted, which does not require specification of patient-specific parameters. Instead, such algorithms learn patterns and biomarkers from a labelled data set. ML has a history of being used for medical applications [8]. Classification algorithms have been shown to be able to predict the presence of irregularities in heart valves [9], arrhythmia [10], and sleep apnea [11] from recorded time domain data. A previous study [12] has applied deep-learning methods to AAA classification, using a synthetic data-set created by varying seven parameters. In [12] accuracies of $\approx 99.9\%$ are reported for binary classification of AAA based on three pressure measurements. These studies motivate the application of ML to detect arterial disease—both stenosis and aneurysms—using only pressure and flow-rate measurements at select locations in the arterial network. A previous proof-of-concept study [13] showed promising results that ML classifiers can detect stenosis in a simple three vessel arterial network using only measurements of pressures and

flow-rates. Here, these ideas are extended to a significantly larger, physiologically realistic, network of the human arterial system. All the ML methods are trained and tested on the virtual healthy subject database proposed in [14], which is augmented to introduce disease into the virtual subjects.

This study is organised as follows. It begins by briefly explaining the healthy VPD proposed in [14]. Modifications to this database to create four different forms of arterial disease are presented next, along with the parameterisation of disease forms. This is followed by presentation of the ML methodology and metrics used for quantification of classification accuracies. Finally, these accuracies are assessed when using different combinations pressure and flow-rate measurements, along with the analysis of patterns and behaviours observed in the ML classifiers.

2 Methodology

The ML algorithms are trained and tested on a data set containing both healthy subjects and diseased patients.

2.1 Healthy subjects

A physiologically realistic VPD containing healthy subjects is created in [14] and forms the starting point of this study. This database is available at [15]. The arterial network contains 71 vessel segments and is shown in Figure 1, along with the locations where disease occurs in high prevalence, and where measurements of pressure and flow-rate can potentially be acquired [14]. The healthy patient database of [14] contains 28,868 VPs and is referred as VPD_H . Disease is introduced into these healthy arterial networks as described next.

2.2 Creation of unhealthy VPDs

2.2.1 Disease forms

The four most common forms of arterial disease are carotid artery stenosis (CAS), subclavian artery stenosis (SAS), peripheral arterial disease (PAD, a form of stenosis), and abdominal aortic aneurysm (AAA) [4, 14, 16–19]. Their prevalence is restricted to the following vessels and shown in Figure 1:

- **CAS** is assumed to only affect the common carotid arteries. For simplification and consistency of notation these vessels are referred to as the **carotid artery chains** (CA_x).
- **SAS** is assumed to affect the first and second subclavian segments. These two chains of vessels (one on the right and left side) are referred to as the **subclavian artery chains** (SA_x).
- **PAD** is assumed to affect the common iliacs; external iliacs; first and second femoral segments; and the first popliteal segments. These chains are referred to as the **peripheral artery chains** (PA_x).
- **AAA** is assumed to affect the first to forth abdominal aorta segment. This chain of vessels is referred to as the **abdominal aortic chain** (AA_x).

It is assumed that each diseased VP has only one of the four forms of arterial disease. Four complementary databases corresponding to VPD_H are constructed, each pertaining to one form of arterial disease. To create the diseased VPD corresponding to CAS, referred to as VPD_{CAS} , for every subject in VPD_H , disease is introduced in CA_x (i.e. the left or right carotid artery). This is achieved by taking the arterial network of a subject from VPD_H , artificially introducing a stenosis in CA_x , and then re-running the pulse-wave propagation model [14] to compute the pressure and flow-rate waveforms. Thus, VPD_{CAS} contains 28,868 VPs with CAS. Similarly, the databases corresponding to SAS, PAD, and AAA are created, and referred to as VPD_{SAS} , VPD_{PAD} , and VPD_{AAA} , respectively. The disease severities, locations, and shapes are varied randomly across these databases as described next.

2.2.2 Parameterisation of diseased vessels

The severity of stenoses (percentage reduction in area) is varied between 50% and 95%. The lower 50% limit is set for the stenoses to be haemodynamically significant [18, 20] and the upper limit of 95% reflects near total occlusion. For aneurysms, based on [21] and [22], an allowable range of AAA severities of 4cm–6cm diameters is chosen. This corresponds to a cross sectional area variation of 12.56cm²–28.27cm². With the abdominal aortic area in the reference network [14] between 1.76cm² and 1.09cm², the corresponding AAA severities are set to vary between 713% (12.56/1.76) and 2,593% (28.27/1.09). With the above ranges, parameterisation of area increase/reduction

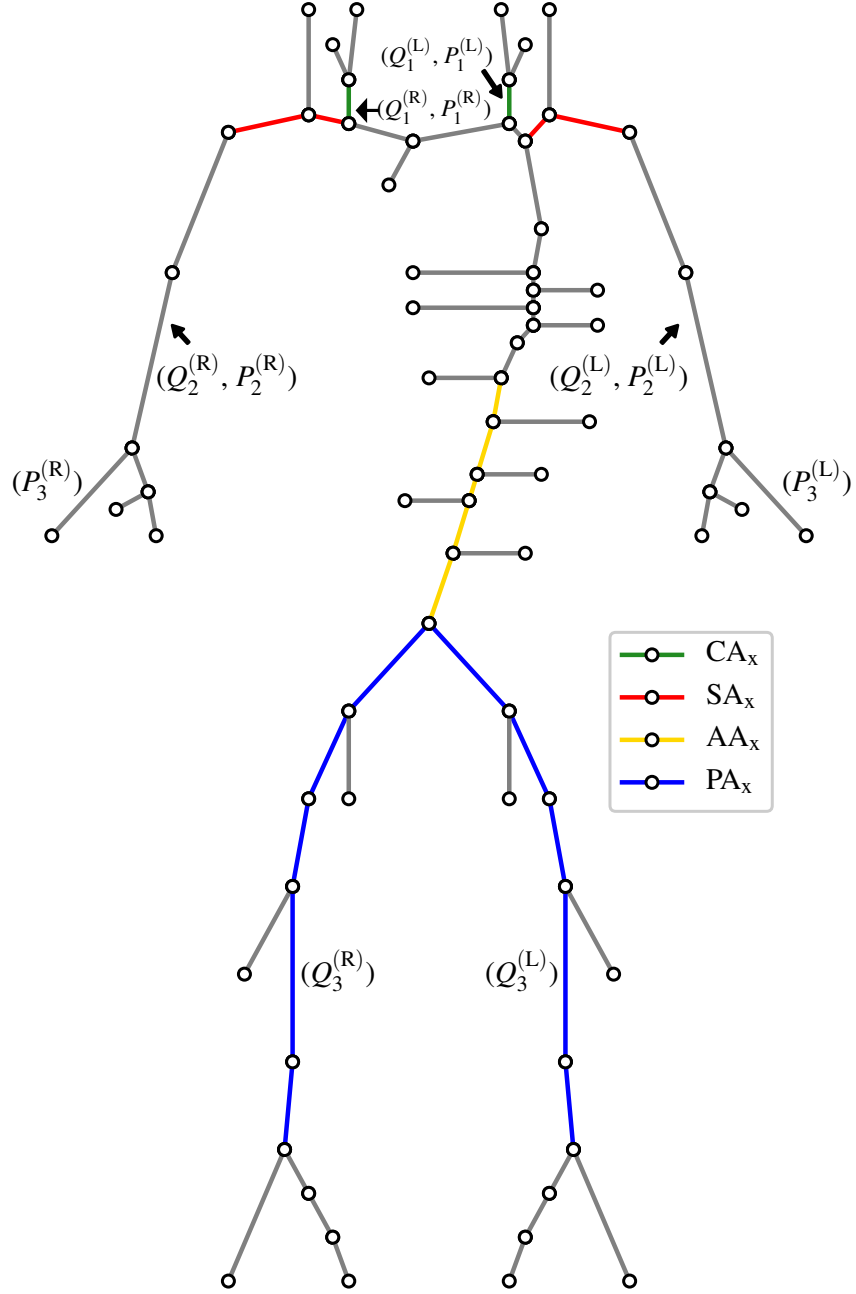


Figure 1: The connectivity of the arterial network, taken from [14]. The location of the four forms of disease (see Section 2.2.1); and six pressure and flow-rate measurements (see section 2.3) are highlighted.

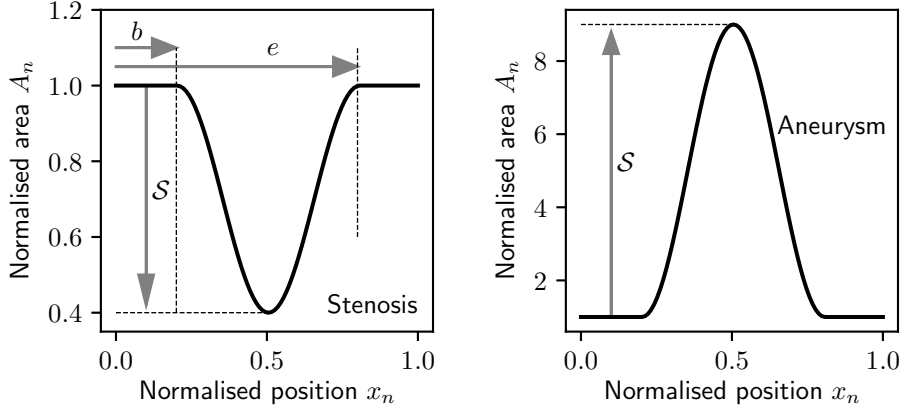


Figure 2: An example of a stenosis of severity 0.6 and aneurysm of severity 8.0 are shown. These disease profiles are created with a start location of 0.2 and an end location of 0.8.

proposed in [13] is adopted, see Figure 2. For a chain of diseased vessels (CA_x , SA_x , PA_x , or AA_x), the normalised area A_n as a function of the normalised x-coordinate, x_n , is represented as:

$$A_n = \begin{cases} \left(1 \mp \frac{\mathcal{S}}{2}\right) \pm \frac{\mathcal{S}}{2} \cos\left(\frac{2(x_n - b)\pi}{e - b}\right) & \text{for } b \leq x_n \leq e \\ 1 & \text{otherwise} \end{cases} \quad (1)$$

where \mathcal{S} represents the severity, b represents the normalised starting location of the disease in the vessel chain, e represents the normalised end location, A_n is normalised with respect to the healthy version of the vessel in VPD_H , and \pm creates an aneurysm or stenosis, respectively. In CA_x , SA_x , and PA_x , the left and right side vessels are chosen with equal probability.

The disease severity \mathcal{S} , start location b , and end location e are assigned uniform distributions based on physical considerations. To sample values for these parameters, a fourth parameter, the reference location of the disease (represented by r) is introduced. This is included to impose a minimum length of 10% of the chain length on the disease profiles. Thus, the parameters for disease are sampled sequentially from uniform distributions within the following bounds:

$$\text{Bounds: } \begin{cases} 0.2 \leq r \leq 0.8, \\ 0.1 \leq b \leq r - 0.05, \\ r + 0.05 \leq e \leq 0.9, \\ \begin{cases} 0.5 \leq \mathcal{S} \leq 0.95 & \text{for stenoses,} \\ 7.13 \leq \mathcal{S} \leq 25.93 & \text{for aneurysms.} \end{cases} \end{cases} \quad (2)$$

Based on the above parameterisation, examples of healthy and diseased SA_x , PA_x , and AA_x area profiles are shown in the left and right columns of Figure 3, respectively.

2.3 Measurements

A review of potential measurements that can be acquired in the network is presented in [14]. Based on this, the locations at which time-varying pressure and flow-rate measurements can be acquired are shown in Figure 1 and described below.

- **Pressure in the carotid and radial arteries** measured using applanation tonometry [23, 24]. To simplify annotation and description the right and left carotid artery pressures are referred as $P_1^{(R)}$ and $P_1^{(L)}$, respectively. Similarly, the radial artery pressures are referred to $P_3^{(R)}$ and $P_3^{(L)}$, respectively.
- **Pressure in the brachial arteries** estimated through reconstruction of finger arterial pressure [25]. The right and left brachial artery pressures are referred to as $P_2^{(R)}$ and $P_2^{(L)}$ respectively.
- **Flow-rate in the carotid, brachial, and femoral arteries** measured using Doppler ultrasound [26–28]. The right and left carotid artery, brachial, and femoral flow-rates are referred to as $Q_1^{(R)}$, $Q_1^{(L)}$; $Q_2^{(R)}$, $Q_2^{(L)}$; and $Q_3^{(R)}$, $Q_3^{(L)}$, respectively.

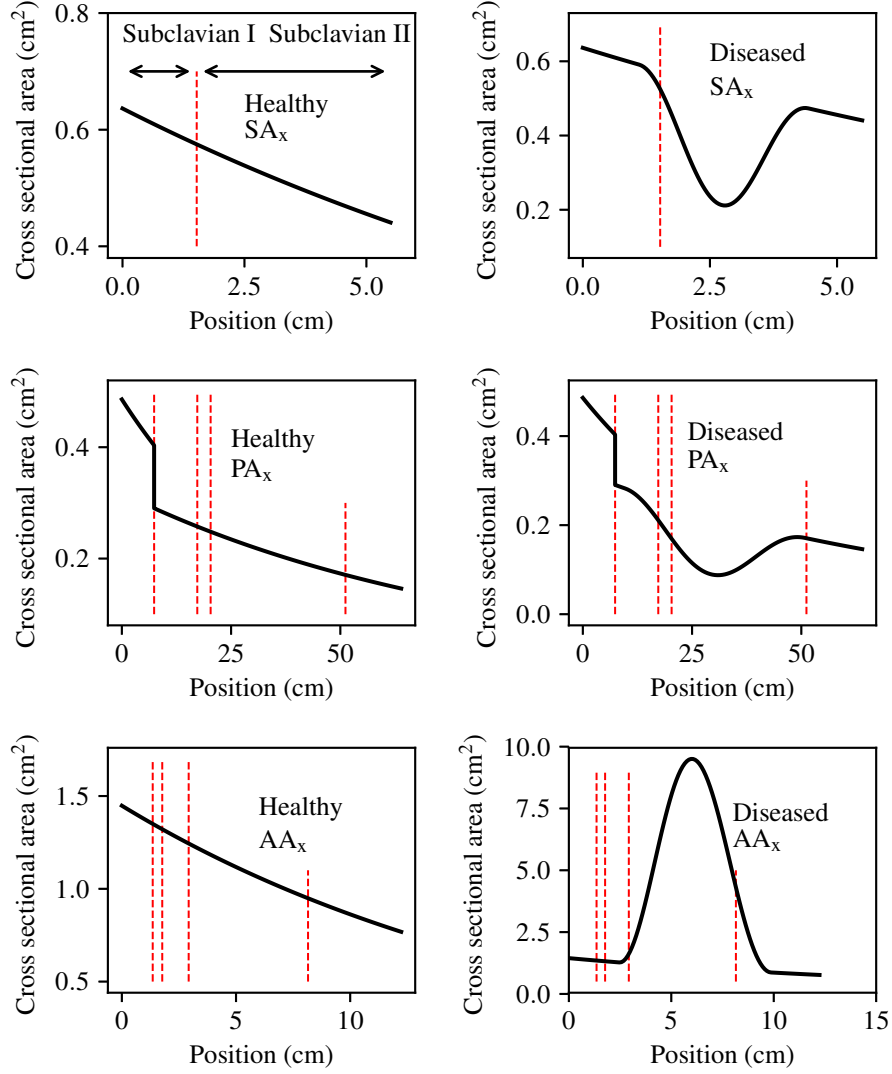


Figure 3: Examples of healthy and diseased SA_x, PA_x, and AA_x area profiles. The geometrical boundaries between vessel segments that form the chains are indicated by red dashed lines.

2.3.1 Provision of measurements to ML classifiers

Unless specified otherwise, the measurements to ML classifiers are bilateral, *i.e.* when Q_1 is specified it is implied that both right and left carotid flow-rates are used:

$$Q_1 = \{Q_1^{(R)}, Q_1^{(L)}\}. \quad (3)$$

There are, therefore, a total of by six bilateral measurements available: three pressure and three flow-rates. To reduce the dimensionality required to describe each pressure or flow-rate measurement, the periodic profiles are described through a Fourier series (FS) representation:

$$u(t) = \sum_{n=0}^N a_n \sin(n\omega t) + b_n \cos(n\omega t), \quad (4)$$

where u represents any pressure or flow-rate profile; a_n and b_n represent the n^{th} sine and cosine FS coefficients, respectively; N represents the truncation order; and $\omega = 2\pi/T$, with T as the time period of the cardiac cycle. It is found in [13] that haemodynamic profiles can be described by a FS truncated at $N = 5$. Thus, each individual measurement is described by 11 FS coefficients, and each bilateral measurement by 22 FS coefficients.

2.4 Machine learning classifiers

A model mapping a vector of input measurements, \mathbf{x} , to a discrete output classification, y , can be described as:

$$y = m(\mathbf{x}) \quad y \in \{\mathcal{C}^{(1)}, \mathcal{C}^{(2)}\}, \quad (5)$$

where $\mathcal{C}^{(j)}$ represents the j^{th} possible classification. In the context of this study, the measured inputs, \mathbf{x} , represents the FS coefficients of a user defined combination of the haemodynamic measurements $\{Q_1, Q_2, Q_3, P_1, P_2, P_3\}$ (see Section 2.3.1) taken from VPs, and the output classification represents the corresponding health of those VPs : $\mathcal{C}^{(1)}$ = ‘healthy’ and $\mathcal{C}^{(2)}$ = ‘diseased’. To account for large differences in magnitudes of the components of \mathbf{x} , they are individually transformed with the Z-score standardisation method [29] to have zero-mean and unit variance.

As previously stated, it assumed that in a patient disease is limited to only one of the four forms. As a first exploratory study, the ML classifiers are created for each form independently. All classifiers are therefore binary (see [13]), *i.e.* four independent classifiers are trained to predict the following questions independently: “*Does a VP belong to VPD_H or VPD_x*”, where x can be either CAS, SAS, PAD, or AAA.

2.4.1 Training and test sets

Each VP in VPD_{CAS}, VPD_{SAS}, VPD_{PAD}, and VPD_{AAA} shares an identical underlying arterial network, apart from the diseased chain, with the corresponding healthy subject in VPD_H. It is, therefore, important to ensure that the same subset of VPs is not included in the both healthy and diseased data sets used for ML classifiers. As each form of disease is mutually exclusive, four independent training and test sets, each corresponding to one form of the disease, are constructed in the following three stages:

- **Step 1:** Half of the available VPs are randomly selected from VPD_H for inclusion within the ML data set; this is referred to as VPD_{H-ML}. The unhealthy VPs corresponding to the remaining unused half are taken from the appropriate unhealthy VPD (VPD_{CAS}, VPD_{SAS}, VPD_{PAD}, or VPD_{AAA}) and incorporated into the ML data set. These data sets are referred to as VPD_{CAS-ML}, VPD_{SAS-ML}, VPD_{PAD-ML}, or VPD_{AAA-ML}.
- **Step 2:** The data sets of Step 1 are combined to create four complete data sets each containing 50% healthy and 50%, unhealthy VPs:
 1. VPD_{H-ML} \cup VPD_{CAS-ML}
 2. VPD_{H-ML} \cup VPD_{SAS-ML}
 3. VPD_{H-ML} \cup VPD_{PAD-ML}
 4. VPD_{H-ML} \cup VPD_{AAA-ML}
- **Step 3:** The four data sets of Step 2 are randomly split into a training set containing 2/3 of all the VPs in the data set, and a test set containing 1/3 of all the VPs.

The performance of all ML classifiers is evaluated using a five fold validation. For each fold, the same data set from Step 2 is used but different subsets are sampled in Step 3 for training and testing.

2.4.2 ML methods

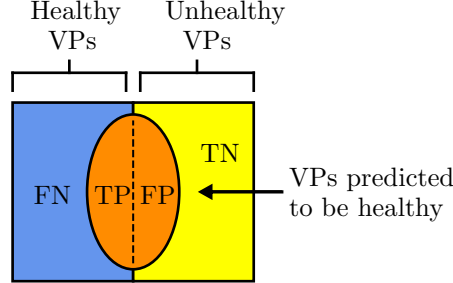
Six different ML methods are employed. These six methods are random forest, gradient boosting, naive Bayes’ , support vector machine, logistic regression , and multi-layer perceptron. Note that the last of these, the multi-layer perceptron, may be considered as a deep learning method. These methods are chosen as they encompass a range of probabilistic and non-probabilistic applications of different modelling approaches, see Table 1, while requiring minimal problem specific optimisation. Since standard versions and implementations of these methods are employed without any modifications, methodological details of these methods are not presented in this study. Instead the reader is referred to the following references for methodological details:

1. Random Forest (RF) [30, 31]
2. Gradient Boosting (GB) [32, 33]
3. Naive Bayes’ (NB) [34, 35]
4. Support Vector Machine (SVM) [36]
5. Logistic Regression (LR) [13, 37, 38]
6. Multi-layer Perceptron (MLP) [39]

All implementations of the above algorithms in the Python package Scikits-learn [40] are used. Some of these methods require optimisation of the hyper-parameters. This is described after presenting performance quantification metrics in the next section.

Modelling approach	Non-probabilistic	Probabilistic
Tree-based	RF	GB
Kernel-based	SVM	
Bayesian		NB
Neuron-based		LR, MLP

Table 1: The four different modelling approaches and how each classification method aligns with these approaches.



$$\text{Recall } (\mathcal{R}) = \text{Sensitivity } (S_e) = \frac{TP}{TP+FN}$$

$$\text{Precision } (\mathcal{P}) = \frac{TP}{TP+FP}$$

$$\text{Specificity } (S_p) = \frac{TN}{TN+FP}$$

$$F_1 = \frac{2\mathcal{P}\mathcal{R}}{\mathcal{P}+\mathcal{R}}$$

Figure 4: The relationship between sensitivity, specificity, recall, and precision. TP: True Positive, representing VPs belonging to a classification correctly identified; FN: False Negative, representing VPs belonging to a classification incorrectly identified; FP: False positive, representing VPs not belonging to a classification incorrectly identified; and TN: True Negative, representing VPs not belonging to a classification correctly identified.

2.4.3 Quantification of results

Classifier performance is assessed by two metrics: *sensitivity* and *specificity* in combination; and the F_1 score. Figure 4 shows the definition of sensitivity, specificity, and F_1 score, along with the related concepts of *precision* and *recall* commonly used in the assessment of classifiers. It is desirable to have both sensitivities and specificities to be high. Similarly, a higher F_1 score is desirable. Since the F_1 score is a single scalar metric that balances both precision and recall, it is a good metric to compare classifiers when tuning the hyper-parameters of ML algorithms. For a discussion on these metrics and their relevance, please refer to [13].

2.5 Hyperparameter optimisation

The architecture of LR, NB, and SVM classifiers can all be considered to be problem independent. While these three algorithms are able to undergo varying levels of problem specific optimisation, the underlying structure of the classifier usually does not change. The architectures of RF, MLP, and GB classifiers, however, are dependent on the specific problem. The architecture choices for the classifiers and associated hyper-parameter optimisation is described next.

2.5.1 LR, SVM, and NB

For LR, the ‘LIBLINEAR’ solver offered by the Scikits-learn [40] package is chosen. In the case of SVM, a kernel is typically chosen to map the input measurements to a higher order feature space [41]. All SVM classifiers use a radial basis function kernel [42]. In the case of NB, the distribution of input measurements across the data set is chosen to be Normal [43].

2.5.2 Random Forest

In the case of RF, the number of trees in the ensemble and the maximum depth of each tree is optimised. To optimise these two hyper-parameters, a grid search is carried out. A grid is constructed by discretising the possible number of trees within the ensemble between 10 and 400 at intervals of 10; and the possible depth of each tree

between 20 and 200 at intervals of 10. RF classifiers are trained for every combination with all six pressure and flow-rate measurements (see Section 2.3.1) across all the four forms of arterial disease. The hyper-parameters describing the architecture that produces the highest F_1 score is found for each form of the disease, and this combination of hyper-parameters is then chosen for all subsequent classifiers. The optimal hyper-parameters for each of the four forms of disease are shown in Table 2, along with the F_1 score achieved by each.

It is unlikely that a single architecture will consistently produce the best results when varying the combination of input measurements. In this study, re-optimisation of the hyper-parameters when varying input measurement combination is avoided to minimise computational cost. It should be noted, however, that further improvements in classification accuracy may be possible with such re-optimisation.

Disease	Trees	Depth	F_1
CAS	100	80	0.8878
SAS	150	80	0.8292
PAD	100	100	0.8935
AAA	100	50	0.9912

Table 2: The hyper-parameters describing the architecture of the RF classifiers that produce the highest F_1 scores, when using all six pressure and flow-rate measurements.

2.5.3 Gradient Boosting

Similar to RF architecture, the GB architecture is optimised for the problem of this study by varying the number of trees within the ensemble and the maximum depth of each tree. A grid search is carried out to find the combination producing the highest F_1 score when using all the six input measurements. It is common for GB classifiers to use weaker, shallower decision trees (relative to RF classifiers) to deliberately create high bias and low variance [44]. The possible depth of each tree is, therefore, discretised between 2 and 20 at intervals of 1. As a high number of trees is not required to compensate for over fitting, contrary to the RF method, the possible number of trees within the ensemble is discretised between 10 and 100 at intervals of 10. The optimal hyper-parameters for each of the four forms of disease are shown in Table 3.

Disease	Trees	Depth	F_1
CAS	100	6	0.9343
SAS	100	7	0.8574
PAD	100	10	0.9187
AAA	80	7	0.9970

Table 3: The hyper-parameters describing the architecture of the GB classifiers that produce the highest F_1 scores, when using all six pressure and flow-rate measurements.

2.5.4 Multi-layer perceptron

In the case of MLP, the number of neurons within each hidden layer, and the number of hidden layers is optimised to create the optimal architecture for the classification problem of this study. For simplicity, it is assumed that all the hidden layers contain an identical number of neurons. Similar to RF and GB, the hyper-parameters that produce the highest F_1 score are found through a grid search. The number of neurons within each layer is discretised between 10 and 200 at intervals of 10, and the number of hidden layers is discretised between 1 and 6 at intervals of 1. The optimal hyper-parameters found for each of the four forms of disease are shown in Table 4. It shows that relative to RF and GB, there is less consistency in the maximum F_1 scores achieved by MLP—it classifies AAA and CAS to high levels of accuracies, but performs relatively poorly for SAS and PAD.

3 Results and discussion

There are 63 possible combinations of input measurements that can be provided to a ML classifier from the six bilateral pressure and flow-rate measurements (see Section 2.3.1). A combination search is performed for each of the four forms of disease. For every combination of input measurements all the six ML classification methods are trained, and then subsequently tested to quantify their performance. The average F_1 score, sensitivity, and specificity for each case across five folds are recorded. Combinations of interest are then further analysed.

Disease	Neurons	Depth	F_1
CAS	60	4	0.7785
SAS	190	2	0.6040
PAD	120	2	0.6681
AAA	30	2	0.9785

Table 4: The hyper-parameters describing the architecture of the MLP classifiers that produce the highest F_1 scores, when using all six pressure and flow-rate measurements.

The full tables of results achieved for CAS, SAS, PAD, and AAA classification are shown in Appendices A, B, C, and D respectively. The F_1 score achieved by each ML method and combination of input measurements are visually shown for CAS, SAS, PAD, and AAA classification in Figures 5, 6, 7, and 8 respectively. They show that for all forms of arterial disease, NB and LR classifiers consistently produce low accuracy. It has previously been shown in the PoC [13] that the partition between the pressure and flow-rate profiles taken from healthy and stenosed patients is likely to be non-linear. The fact that LR consistently produces low accuracy results supports this finding, as LR is the only linear classification method used. The finding that NB classifiers also produce low accuracy classification is also consistent with the results of the PoC [13], which found that the NB method is poorly suited to the problem of distinguishing between hemodynamic profiles. On the contrary, across all the four forms of disease, the tree based methods (RF and GB) consistently produce high accuracy results. This finding is in contradiction to the finding in the PoC [13], and is likely due to the inadequate architecture optimisation or because of the unsuitability of RF on a smaller network used in the PoC [13]. The fact that both RF and GB classifiers are producing high accuracy classification in this study suggests that not only are tree based methods well suited to distinguishing between haemodynamic profiles, but also emphasises the importance of adequate architecture optimisation.

There is less consistency in the results achieved by SVM and MLP classifiers when detecting different forms of disease. SVM classifiers produce accuracies comparable with RF and GB classifiers in the case of AAA detection, however low accuracy results for the three other forms of disease. MLP classifiers produce accuracies comparable with RF and GB classifiers in the case of CAS and AAA detection, however relatively low accuracy results for SS and PAD classification. Overall, it is found that tree-based methods of RF and GB perform best, with GB performance slightly superior to that of RF.

3.1 Measurement combinations

To investigate the importance of both the number of input measurements provided to the ML algorithms and the specific combination of measurements, the average F_1 scores achieved by all classifiers when providing only one, two, three, four, five, or six input measurements are found. In each case, the specific combinations that achieve the maximum and minimum F_1 scores are also recorded. These results for different forms of disease are presented next.

3.1.1 CAS classification

The average, maximum and minimum F_1 score achieved when providing different number of input measurements for CAS classification are shown in Figure 9. It shows that NB, LR, and SVM classifiers consistently produce an F_1 score of approximately 0.5, which is comparable to naive classification, *i.e.* randomly assigning the health of VPs with an equal probability to each outcome. SVM performs slightly better with F_1 scores averaging 0.5 – 0.6. The other three classification methods (RF, MLP, and GB) perform significantly better with F_1 scores generally averaging between 0.7 and 0.95 and showing a clear increase in the average F_1 score as the number of input measurements increases. While the average and minimum F_1 score achieved by RF and GB classifiers continuously increases, the maximum F_1 score achieved can be seen to quickly reach a plateau (at one input measurement for RF, and three input measurements for GB). For a fixed number of measurements, the wide range of F_1 scores in Figure 9 across all classifiers suggests that specific combinations of measurements may be more important than others for optimal classification. To explore this further, the combinations of input measurements that produce the highest F_1 scores and the corresponding accuracies when employing the RF and GB methods are shown in Table 5. Two observations are made from this table. First that for a fixed number of measurements, the best combinations are not identical for the two methods. For example, when two measurements are used the best combination for RF is (Q_2, Q_1) while the best combination for GB is (P_2, P_1) . This suggests that the best combination of measurements is likely dependent on the particular ML method chosen. Second, some patterns stand out with respect to which measurements may be more informative than others. For example, across the Table 5 Q_1 appears in 11 out of 12 combinations and P_1 appears in 8 out of 12 combinations. This suggests that Q_1 is most informative about identifying the presence of CAS followed by P_1 . Physiologically, this is not surprising as Q_1 and P_1 are flow-rates

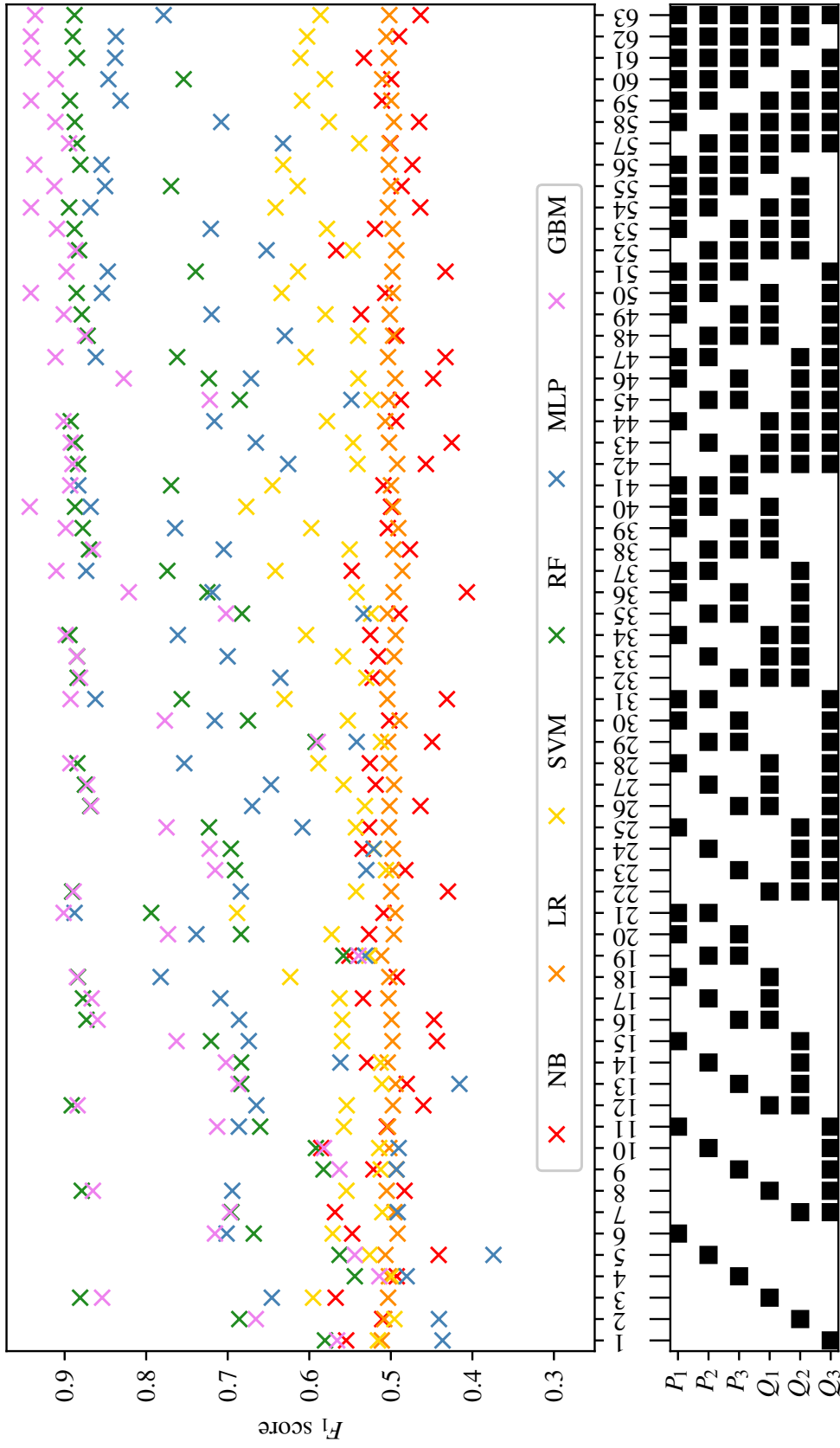


Figure 5: The F_1 scores achieved for CAS using each combination of bilateral input measurements are shown. Measurements included within each combination are highlighted with a black square.

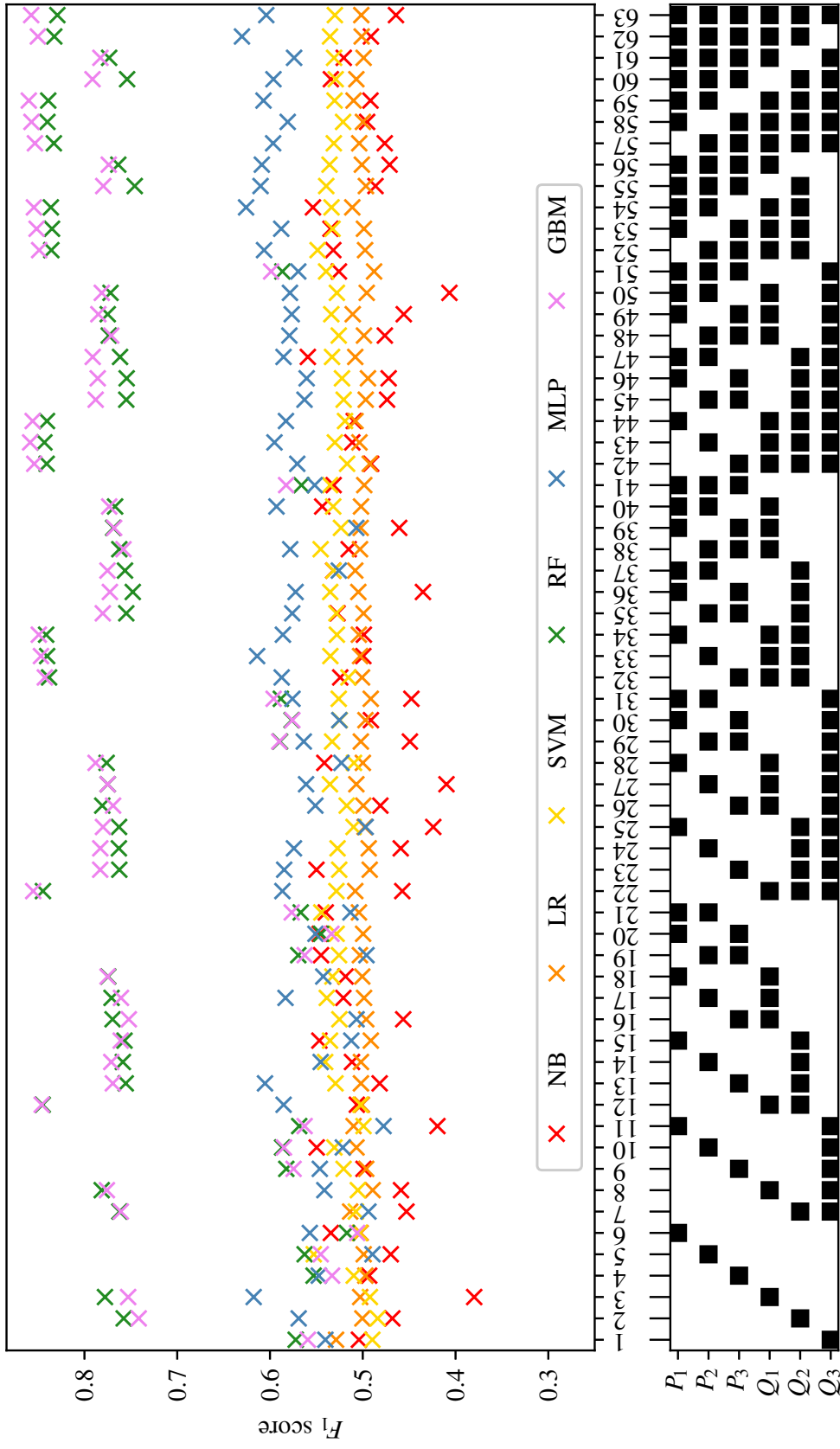


Figure 6: The F_1 scores achieved for SAS using each combination of bilateral input measurements are shown. Measurements included within each combination are highlighted with a black square.

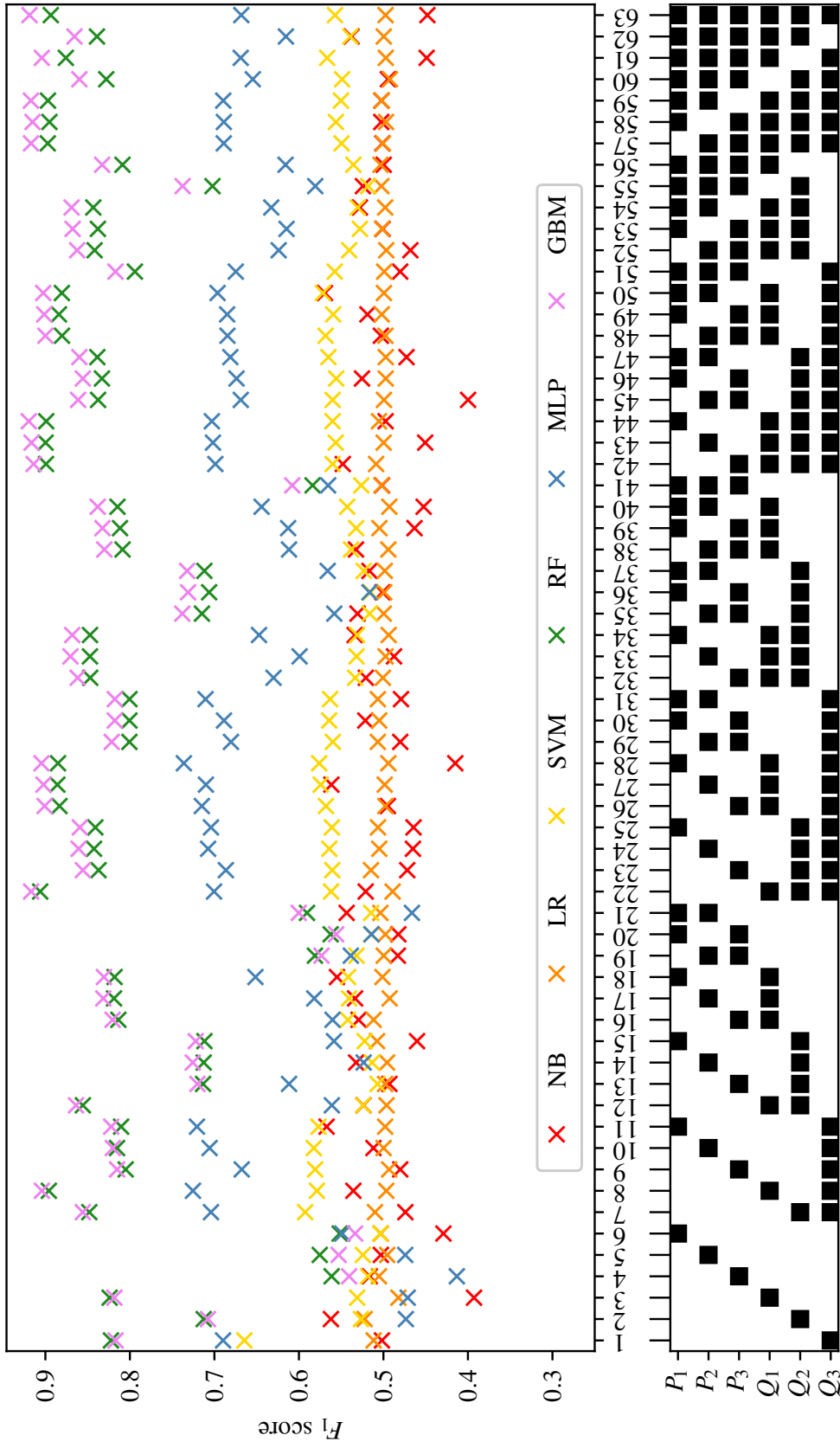


Figure 7: The F_1 scores achieved for PAD using each combination of bilateral input measurements are shown. Measurements included within each combination are highlighted with a black square.

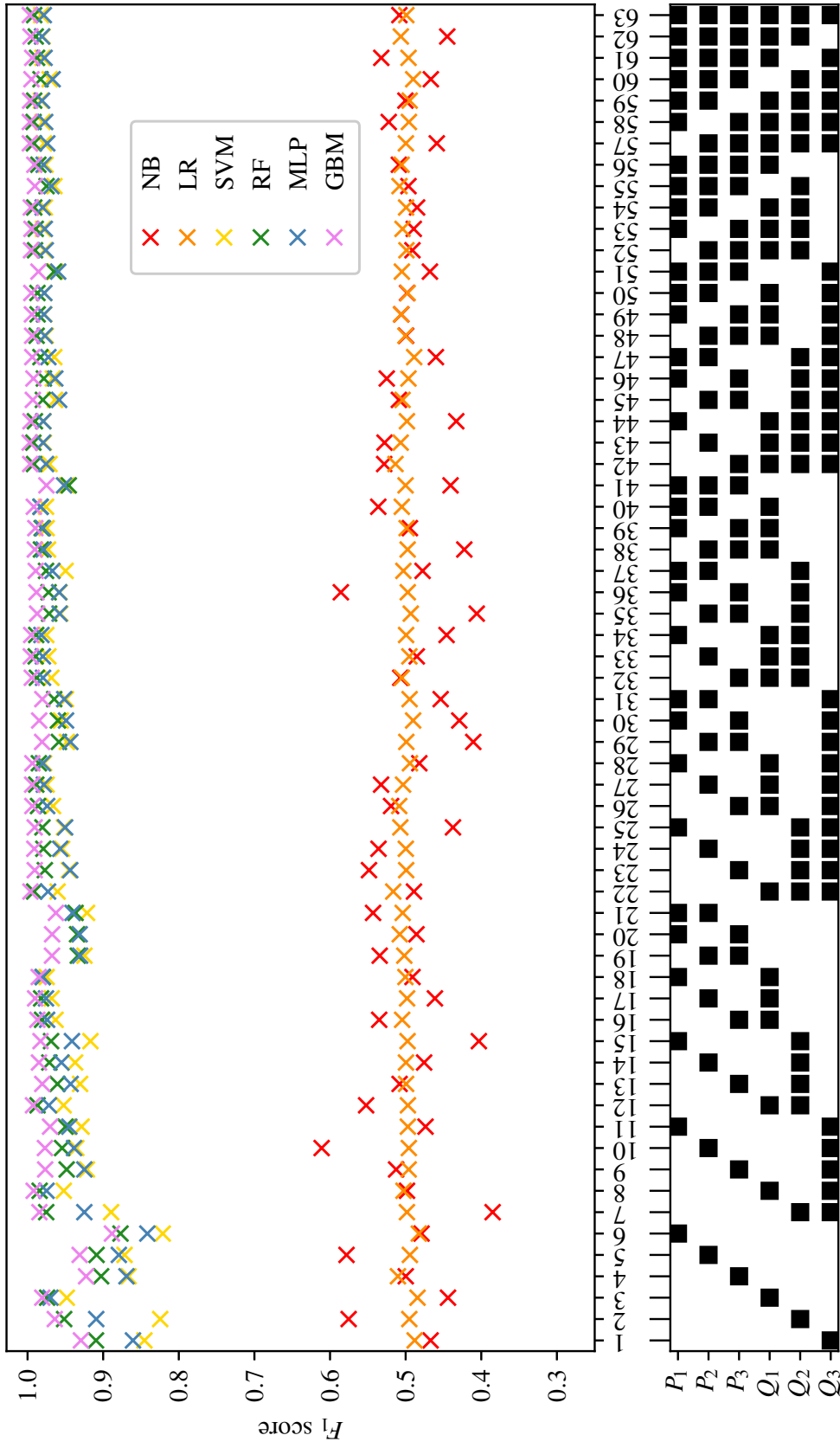


Figure 8: The F_1 scores achieved for AAA using each combination of bilateral input measurements are shown. Measurements included within each combination are highlighted with a black square.

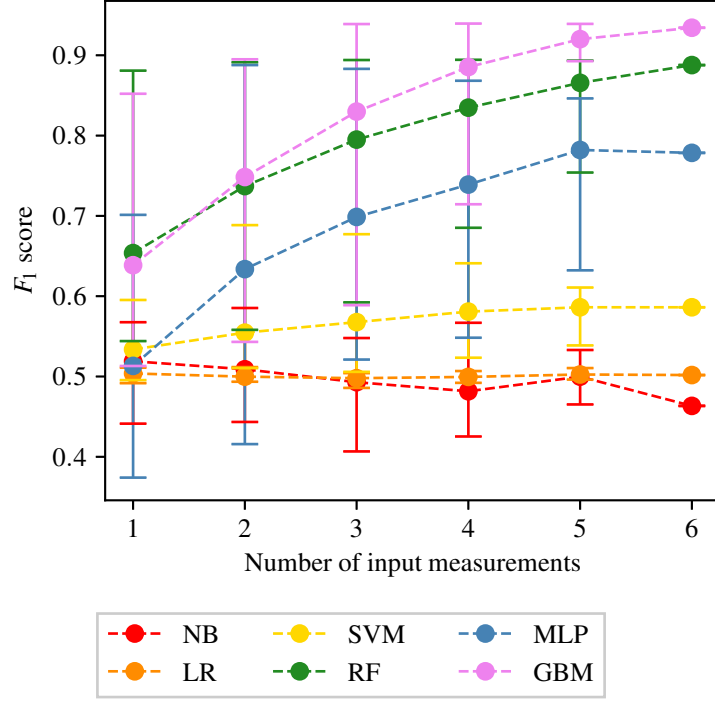


Figure 9: The average, maximum, and minimum F_1 score achieved by all classifiers trained using different numbers of input measurements are shown for carotid artery stenosis classification. The central markers represent the average score achieved, while the error bars indicate the upper and lower limits.

and pressures in the carotid arteries and the disease under consideration is carotid artery stenosis. It is encouraging that the ML methods are indeed placing more importance to the relevant physiological measurements. In fact, it is remarkable that RF and GB both achieve F_1 scores above 0.85 and sensitivities and specificities larger than 85% with only this measurement. Also notable is that these accuracies can be taken to beyond 93% (see GB row for 3 measurements in Table 5) when adding 2 more measurements as long as the additional two measurements are carefully chosen.

An interesting pattern to note is that while the average and minimum F_1 score achieved by MLP classifiers continuously increases in Figure 9, the maximum F_1 score decreases beyond three input measurements. The maximum F_1 scores achieved by MLP classifiers, and the corresponding sensitivities and specificities, when using three to six input measurements are shown in Table 6. It shows that the decrease in F_1 scores is also accompanied by an associated decrease in both the sensitivities and specificities, as opposed to the balance between them (increase in sensitivity and decrease in specificity and vice versa). This behaviour is unusual as intuitively more input measurements should generally provide more information. This finding may suggest that MLP classifiers are able to extract maximum information from the haemodynamic profiles when using as little as three input measurements, and may be susceptible to over fitting when using more than three measurements, thereby leading to less generalisation capabilities and consequently decreased accuracies.

3.1.2 SAS classification

The results of the analysis for SAS classification are shown in Figure 10. As is seen in the case of CAS classification, Figure 10 shows that NB, LR, and SVM classifiers consistently produce accuracies comparable to naive classification, irrespective of the number of input measurements used. A clear difference between Figures 9 and 10 is the accuracy achieved by MLP classifiers. Compared to the CAS case, the MLP performance is further degraded for SAS, while still being better than NB, LR, and SVM, although only marginally.

A high degree of similarity can be seen between the behaviours of RF and GB classifiers for CAS and SAS. Figure 10 shows that the average and minimum F_1 score achieved by RF and GB classifiers continuously increases as the number of input measurements used increases. The maximum F_1 score achieved is seen to quickly reach an asymptotic limit (at three input measurements for both RF and GB classifiers). Peak F_1 score of approximately 0.85 is achieved by GB, along with sensitivities and specificities higher than 85%.

The combination of input measurements that produce the highest F_1 scores and the corresponding accuracies are shown in Table 7. It shows a higher degree of consistency between the best combinations for the two methods relative to the case for CAS, i.e. the best combinations are generally identical (or with minimal differences) between

Number of input measurements	Method	Combination	F_1 score	Sens.	Spec.
1	RF	(Q_1)	0.8809	0.8704	0.8893
	GB	(Q_1)	0.8521	0.8547	0.8502
2	RF	(Q_2, Q_1)	0.8913	0.8765	0.9032
	GB	(P_2, P_1)	0.8950	0.9026	0.8889
3	RF	(Q_2, Q_1, P_1)	0.8941	0.8825	0.9035
	GB	(Q_1, P_2, P_1)	0.9389	0.9433	0.9351
4	RF	(Q_2, Q_1, P_2, P_1)	0.8944	0.8858	0.9015
	GB	(Q_3, Q_1, P_2, P_1)	0.9395	0.9417	0.9376
5	RF	$(Q_3, Q_2, Q_1, P_2, P_1)$	0.8934	0.8858	0.8996
	GB	$(Q_2, Q_1, P_3, P_2, P_1)$	0.9391	0.9416	0.9370
6	RF	$(Q_3, Q_2, Q_1, P_3, P_2, P_1)$	0.8878	0.8747	0.8984
	GB	$(Q_3, Q_2, Q_1, P_3, P_2, P_1)$	0.9343	0.9364	0.9325

Table 5: The combinations of input measurements that produce the maximum F_1 scores when providing one to six input measurements and employing the RF and GB methods to detect CAS. The corresponding sensitivities and specificities are also included.

Number of input measurements	Combination	F_1 score	Sensitivity	Specificity
3	(P_3, P_2, P_1)	0.8831	0.8731	0.8911
4	(Q_3, Q_1, P_2, P_1)	0.8683	0.8538	0.8545
5	$(Q_3, Q_2, P_3, P_2, P_1)$	0.8463	0.8308	0.8577
6	$(Q_3, Q_2, Q_1, P_3, P_2, P_1)$	0.7785	0.7916	0.7703

Table 6: The combinations of input measurements that produce the maximum F_1 scores when providing three to six input measurements and employing the MLP method to detect CAS. The corresponding sensitivities and specificities are also included.

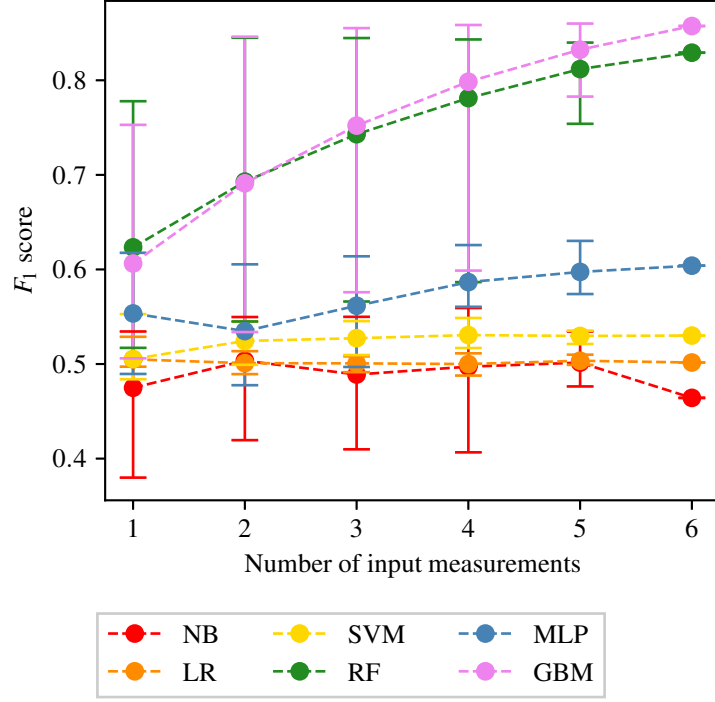


Figure 10: The average, maximum, and minimum F_1 score achieved by all classifiers trained using different numbers of input measurements are shown for SAS classification. The central markers represent the average score achieved, while the error bars indicate the upper and lower limits.

RF and GB. It also shows that Q_1 is particularly informative, with this measurement appearing in all of the best combinations. Physiologically this may be due to its proximity to the disease location.

3.1.3 PAD classification

The results for PAD classification are shown in Figure 11. Comparing Figures 10 and 11, a high degree of similarity is seen between the behaviours of SAS and PAD classification. As is previously seen for SAS classification, Figure 11 shows that the NB, LR, and SVM methods are all consistently producing accuracies comparable to naive classification. While the MLP method performs slightly better than the naive classification, the accuracy still remains relatively low. High accuracy can be seen in Figure 11 for the two tree based methods of RF and GB. As has been previously seen for CAS and SAS, while the average and minimum F_1 score achieved by the RF and GB methods increases as the number of input measurements increases, the maximum F_1 score achieved quickly reaches an asymptotic limit (at 3 input measurements for both the RF and GB methods).

The combination of input measurements that produce the highest F_1 scores for PAD classification when employing the RF and GB methods are shown in Table 8. Table 8 not only shows good consistency between the combinations of input measurements that produce the highest F_1 scores when employing each of the two ML methods, but also good agreement with the combinations presented in Table 7. Very similar combinations of input measurements (with some minor differences) can be seen to produce the highest F_1 score when providing all numbers of input measurements. As has previously been observed in Tables 5 and 7, the input measurement Q_1 appears to be most informative, appearing in all the best scoring classifiers. Since the location of Q_1 is far from the location of disease, it is not obvious why this measurement is particularly informative of PAD.

3.1.4 AAA classification

The results for AAA classification are shown in Figure 12. As has been previously seen for all of the three other forms of disease the NB, and LR classifiers consistently produce accuracies comparable to naive classification, irrespective of the number of input measurements used. The consistency of this finding (as seen in Figures 9, 10, and 11), irrespective of the form of disease being classified, highlights both the importance of non-linear partitions between healthy and unhealthy VPs and the unsuitability of the NB method for distinction between haemodynamic profiles.

In the case of AAA classification the SVM, RF, MLP, and GB methods consistently produce good accuracies. Figure 12 shows that these methods produce high accuracies even with a single input measurement. While there

Number of input measurements	Method	Combination	F_1 score	Sens.	Spec.
1	RF	(Q_1)	0.7779	0.7582	0.7905
	GB	(Q_1)	0.7529	0.7224	0.7714
2	RF	(Q_2, Q_1)	0.8450	0.8374	0.8507
	GB	(Q_2, Q_1)	0.8461	0.8293	0.8585
3	RF	(Q_3, Q_2, Q_1)	0.8447	0.8271	0.8576
	GB	(Q_3, Q_2, Q_1)	0.8552	0.8453	0.8626
4	RF	(Q_3, Q_2, Q_1, P_2)	0.8432	0.8303	0.8527
	GB	(Q_3, Q_2, Q_1, P_2)	0.8585	0.8487	0.8660
5	RF	$(Q_3, Q_2, Q_1, P_3, P_1)$	0.8399	0.8256	0.8504
	GB	$(Q_3, Q_2, Q_1, P_2, P_1)$	0.8600	0.8525	0.8657
6	RF	$(Q_3, Q_2, Q_1, P_3, P_2, P_1)$	0.8292	0.8102	0.8427
	GB	$(Q_3, Q_2, Q_1, P_3, P_2, P_1)$	0.8574	0.8504	0.8627

Table 7: The combinations of input measurements that produce the maximum F_1 scores when providing one to six input measurements and employing the RF and GB methods to detect SAS. The corresponding sensitivities and specificities are also included.

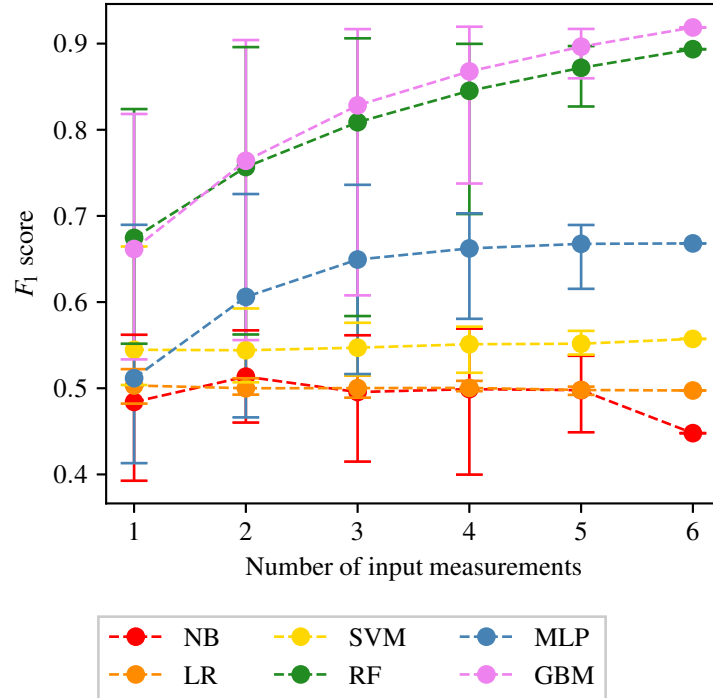


Figure 11: The average, maximum, and minimum F_1 score achieved by all classifiers trained using different numbers of input measurements are shown for PAD classification. The central markers represent the average score achieved, while the error bars indicate the upper and lower limits.

Number of input measurements	Method	Combination	F_1 score	Sens.	Spec.
1	RF	(Q_1)	0.8240	0.8959	0.8320
	GB	(Q_1)	0.8183	0.8126	0.8214
2	RF	(Q_3, Q_1)	0.8140	0.8825	0.9068
	GB	(Q_3, Q_1)	0.9041	0.8950	0.9117
3	RF	(Q_3, Q_2, Q_1)	0.9061	0.8885	0.9208
	GB	(Q_3, Q_2, Q_1)	0.9168	0.9055	0.9265
4	RF	(Q_3, Q_2, Q_1, P_2)	0.8997	0.8868	0.9104
	GB	(Q_3, Q_2, Q_1, P_1)	0.9196	0.9068	0.9306
5	RF	$(Q_3, Q_2, Q_1, P_3, P_2)$	0.8971	0.8802	0.9110
	GB	$(Q_3, Q_2, Q_1, P_2, P_1)$	0.9170	0.9041	0.9281
6	RF	$(Q_3, Q_2, Q_1, P_3, P_2, P_1)$	0.8935	0.8813	0.9035
	GB	$(Q_3, Q_2, Q_1, P_3, P_2, P_1)$	0.9187	0.9102	0.9261

Table 8: The combinations of input measurements that produce the maximum F_1 scores when providing one to six input measurements and employing the RF and GB methods to detect PAD. The corresponding sensitivities and specificities are also included.

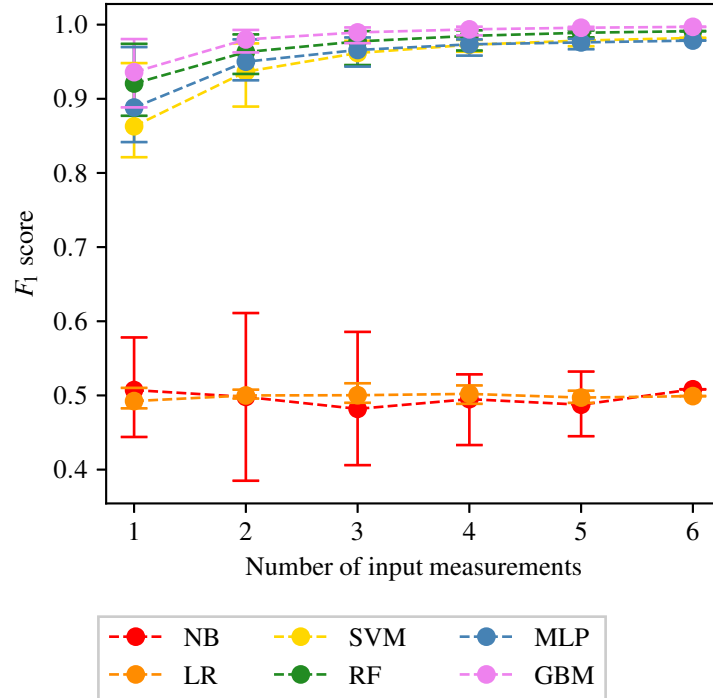


Figure 12: The average, maximum, and minimum F_1 score achieved by all classifiers trained using different numbers of input measurements are shown for AAA classification. The central markers represent the average score achieved, while the error bars indicate the upper and lower limits.

Number of input measurements	Method	Combination	F_1 score	Sens.	Spec.
1	RF	(Q_1)	0.9741	0.9654	0.9825
	GB	(Q_1)	0.9805	0.9799	0.9811
2	RF	(Q_2, Q_1)	0.9868	0.9810	0.9926
	GB	(Q_2, Q_1)	0.9928	0.9919	0.9938
3	RF	(Q_3, Q_2, Q_1)	0.9912	0.9864	0.9961
	GB	(Q_3, Q_2, Q_1)	0.9962	0.9954	0.9970
4	RF	(Q_3, Q_2, Q_1, P_2)	0.9923	0.9879	0.9967
	GB	(Q_3, Q_2, Q_1, P_2)	0.9972	0.9959	0.9986
5	RF	$(Q_3, Q_2, Q_1, P_3, P_1)$	0.9920	0.9873	0.9967
	GB	$(Q_3, Q_2, Q_1, P_3, P_2)$	0.9970	0.9959	0.9981
		$(Q_3, Q_2, Q_1, P_3, P_1)$		0.9963	0.9978
6	RF	$(Q_3, Q_2, Q_1, P_3, P_2, P_1)$	0.9912	0.9861	0.9964
	GB		0.9970	0.9959	0.9981

Table 9: The combinations of input measurements that produce the maximum F_1 scores when providing one to six input measurements and employing the RF and GB methods to detect AAA. The corresponding sensitivities and specificities are also included.

is some increase in the average F_1 score as the number of input measurements increases, due to the very high initial average F_1 score achieved (when using a single input measurement) this increase is limited (as the F_1 score can not exceed 1). Two possible reasons of the higher accuracies in aneurysm classification relative to stenosis classification are:

- Aneurysms, owing to an increase in area as opposed to decrease in the area for stenoses, may actually produce more significant or consistent biomarkers in the pressure and flow-rate profiles. This hypothesis is supported by [45], which found that even low severity AAAs have a global impact on the pressure and flow-rate profiles.
- While the severities of aneurysms cannot be directly compared to severities of stenosis, it may be that the severity of aneurysms in VPD_{AAA} are disproportionately large relative to the severities of stenoses. The significance of any indicative biomarkers introduced into pressure and flow-rate profiles is likely to be proportional to the severity of the change in area. This implies that the increase in vessel area of 712%–2,593% in VPD_{AAA} is perhaps on the extreme end of aneurysm severity, thereby making the classifications relatively easier. This is further explored in section 3.4.

The combination of input measurements that produce the highest F_1 scores when providing one to six input measurements and employing the RF and GB methods are shown for AAA classification in Table 9. It shows that F_1 scores range from 0.97–0.997 and sensitivities and specificities range from 99% to 99.8%. Due to the high accuracies across all the number of measurements, the analysis of specific combinations is not very meaningful. However, the measurement Q_1 again appears in all the best combinations. It should also be noted that the high accuracies for AAA classification are also consistent with those reported in [12], where deep-learning methods are applied on a VPD created by varying seven network parameters, and classification accuracies of $\approx 99.9\%$ are reported.

Overall, the results show that the physiological changes to the waveforms induced by both stenosis and aneurysms [7, 45] are well captured by the data-driven machine learning methods.

3.2 Importance of carotid artery flow-rate

Appendices A–D, along with the above analysis show that classifiers trained using flow-rates in the common carotid arteries (Q_1) consistently produce the highest accuracy. To analyse this further, the F_1 scores of classifiers with combinations that include and exclude Q_1 are separated and compared for CAS, SAS, PAD, and AAA in Figures 13, 14, 15, and 16 respectively. These figures show the the histograms of the F_1 scores, i.e. the number of occurrences/classifiers/combinations including and excluding Q_1 against F_1 score buckets. For each disease form, results are only shown for the classification methods that consistently produce good results for the corresponding disease form. The figures show a clear positive shift in the histograms when Q_1 is included, pointing to the particularly informative nature of Q_1 . Other behaviours observed from these figures are:

- While there is generally an increase in F_1 score when including Q_1 , it is also simultaneously observed that the maximum accuracies are relatively less sensitive to the inclusion of Q_1 .

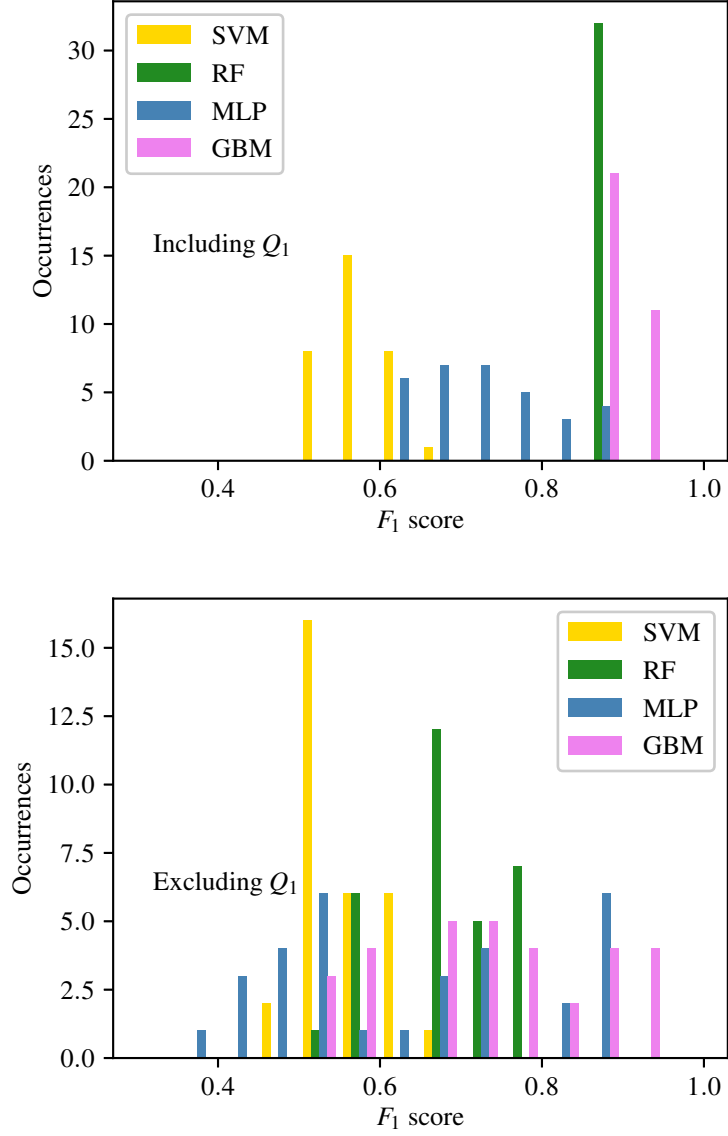


Figure 13: The histograms of the F_1 scores achieved for CAS classification are shown for all input measurement combinations that include Q_1 in the upper plot, and exclude Q_1 in the lower plot.

- The greatest distinction between F_1 scores when including or excluding Q_1 is seen for CAS classification when using the RF method. There is no overlap between the two RF histograms in Figure 13.
- Observing the lower plots in Figures 14 and 15, a clear subgroup of low-accuracy classifiers can be seen when excluding Q_1 for SAS and PAD, which does not exist when including Q_1 .

3.3 Feature importance

An important aspect of the GB method is that the measurement importance, which determines the influence that individual measurements have towards classification, can be computed. This split-improvement feature importance [46] of a feature can be thought of as the contribution of that feature to the total information gain achieved in a decision tree, averaged across all the trees in the ensemble. A high feature importance suggests that the given feature is contributing heavily to the classification accuracies achieved. As the features provided to the GB classifiers are the FS coefficients describing the haemodynamic profiles, the total importance of each bilateral pressure or flow-rate measurement is found by summing the feature importance of the associated 22 FS coefficients. The total importance of each input measurement for each disease form is shown in Table 10. Three important observations from this table are:

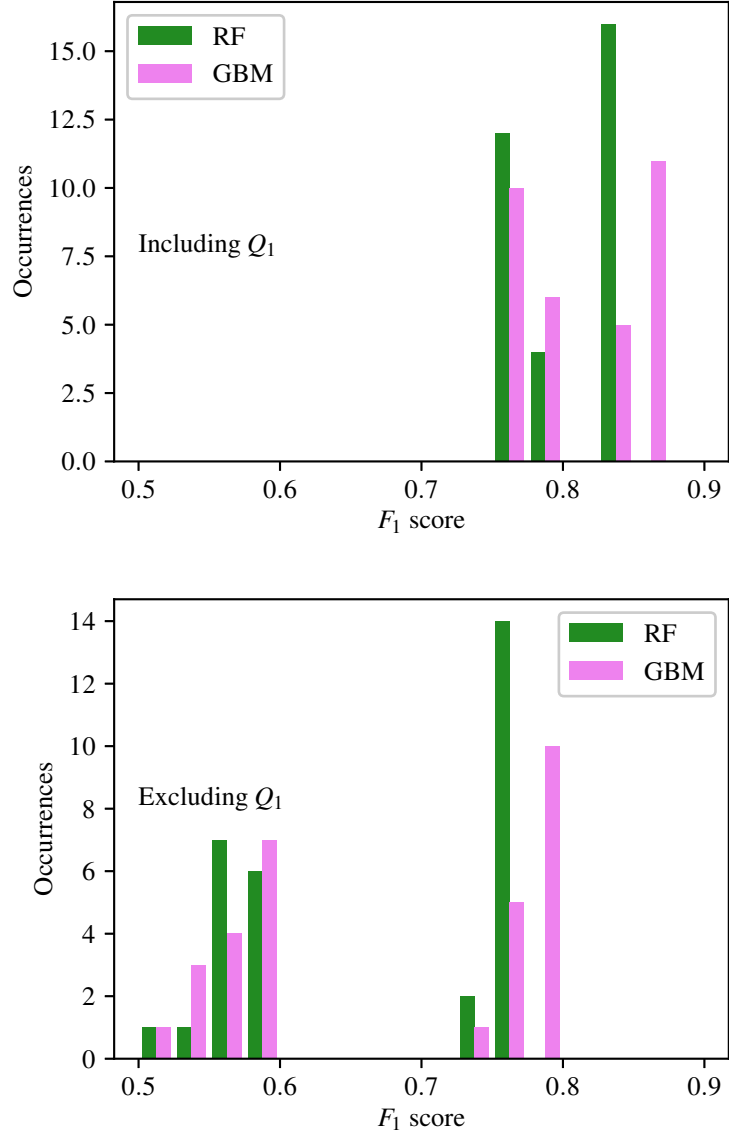


Figure 14: The histograms of the F_1 scores achieved for SAS classification are shown for all input measurement combinations that include Q_1 in the upper plot, and exclude Q_1 in the lower plot.

	Q_1 (%)	Q_2 (%)	Q_3 (%)	P_1 (%)	P_2 (%)	P_3 (%)
CAS	67.38	8.02	3.89	11.07	7.692	1.93
SAS	41.90	29.98	8.40	6.80	5.97	6.921
PAD	38.01	15.98	31.11	4.62	4.63	5.62
AAA	69.34	19.10	4.95	2.41	2.61	1.55

Table 10: The total importance of each input measurement, based on the GB classifiers provided with all six measurements.

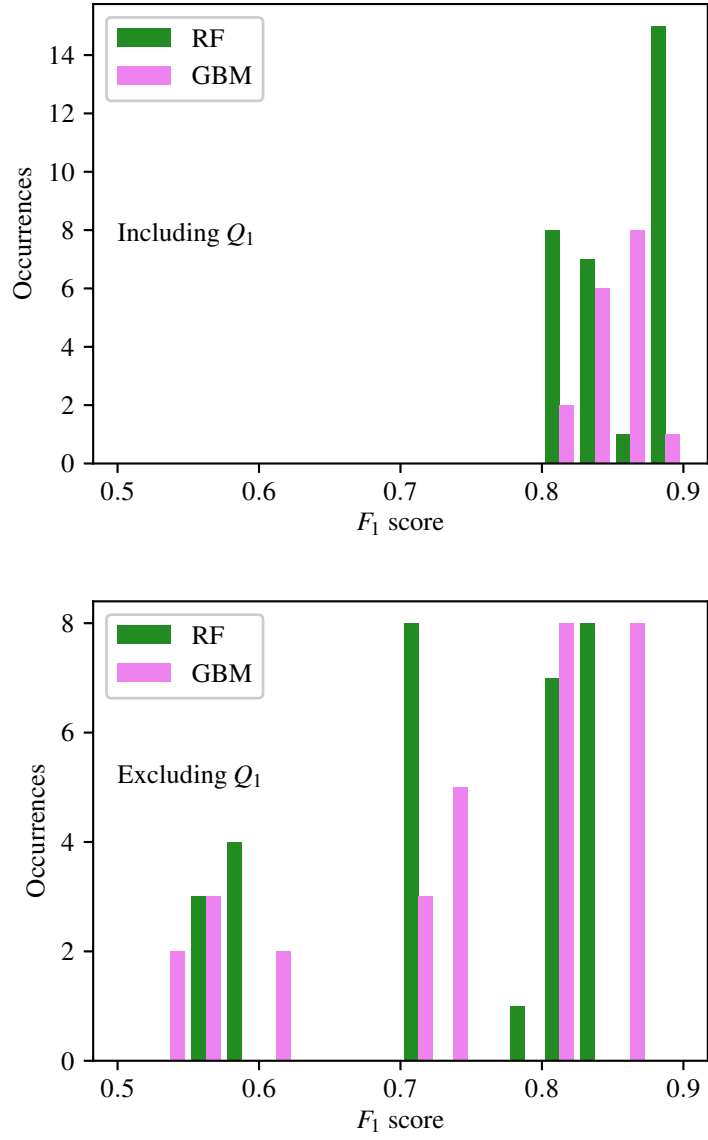


Figure 15: The histograms of the F_1 scores achieved for PAD classification are shown for all input measurement combinations that include Q_1 in the upper plot, and exclude Q_1 in the lower plot.

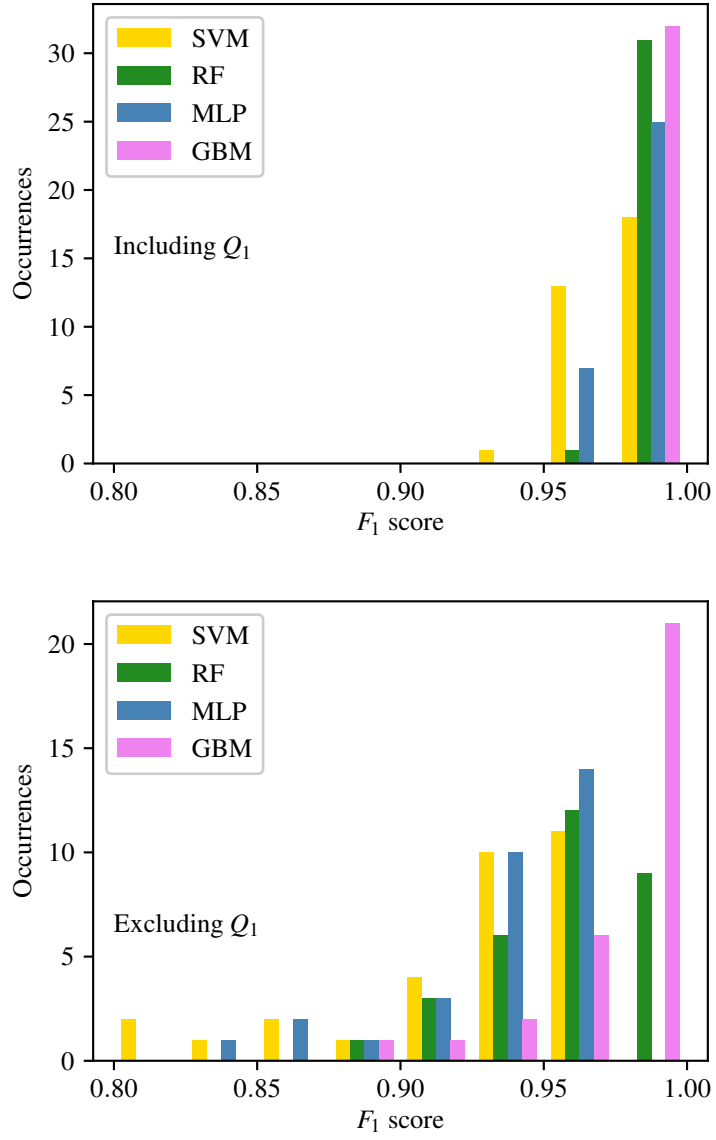


Figure 16: The histograms of the F_1 scores achieved for AAA classification are shown for all input measurement combinations that include Q_1 in the upper plot, and exclude Q_1 in the lower plot.

- The input measurement Q_1 consistently produces the highest importance for all forms of disease. This finding supports the findings of Section 3.2.
- The importance of each input measurement changes between disease forms based on the spatial proximity to the disease location. Generally, the measurements in close proximity to the disease location have higher importance. For example the importance of Q_3 (flow-rate in the femoral arteries) is highest for PAD classification (see Figure 1 for locations of disease and measurements). Similarly, P_1 (pressure in carotid arteries) has highest importance for CAS and SAS.
- The feature importances, when viewed in collection, also shed some light on why Q_1 is important for SAS and PAD even though the measurement location is far from the disease location. For SAS, the two most informative measurements are Q_1 and Q_2 , and for PAD these are Q_1 and Q_3 . From Figure 1, it is clear that these combinations form pairs of flow-rates before and after/at the disease location. Thus the measurement locations bound the disease location to provide more information on the presence of disease.

3.4 Lower severity aneurysms

In Section 3.1.4 it is found that AAAs can be classified to a very high levels of accuracy with only one input measurement. Whether these accuracies are affected when lower severity aneurysms are considered is assessed here. For this assessment, a new lower severity AAA VPD, referred to as VPD_{AAA-L} , is created in an identical manner to the other diseased databases (see section 2.2), with the following two differences:

- The severity of aneurysms introduced into the virtual subjects (see Section 2.2.2) is sampled from a uniform distribution bounded as follows: $3.0 \leq \mathcal{S}_{aneurysm} \leq 7.0$.
- To reduce the computational expense associated with the creation of virtual patients, the size of VPD_{AAA-L} is restricted to 5,000 VPs.

A combination search is carried out with only the GB method as it is the best overall method. The F_1 scores, sensitivities, and specificities achieved by all the measurement combinations are presented in Appendix E. For comparison, the GB F_1 scores for all forms of disease (including AAA-L) are shown in Appendix F. The ratios of the GB F_1 scores achieved for AAA-L classification relative to AAA classification are shown in Figure 17. The observations from this figure are:

- The F_1 scores for AAA-L classification are consistently lower (ranging from 1% to 10% lower) than that for AAA classification. This finding supports the physiological expectation that the significance of biomarkers in pressure and flow-rate profiles is proportion to the severity.
- The ratios of F_1 scores are lowest for combinations of inputs that predominantly rely on pressure measurements. This suggests that pressure measurements are, in general, less informative about disease severity. This is in support of the, generally, lower feature importance of pressure measurements in Table 10.
- The F_1 score ratios are highest for input combinations that include Q_1 . This finding further suggests that Q_1 contains consistent biomarkers.
- The ratios range between 0.9 and 0.99, implying a maximum degradation of only 10% relative to high-severity classification accuracies. Thus, even in the low-severity aneurysms many combinations of classifiers achieve F_1 scores higher than 0.95 and corresponding sensitivities and specificities larger than 95%.

3.5 Unilateral aneurysm measurement tests

Hitherto, all ML classifiers used bilateral measurements, *i.e.* both the right and left instances of each measurement were simultaneously provided. Here, the ability of unilateral measurements, *i.e.* only the right or left instance of a measurement, to detect AAAs is assessed. This analysis is restricted to the GB method as it consistently outperforms other methods. GB classifiers are trained and tested to detect AAAs using four different unilateral measurements:

- **Flow-rate in the right carotid artery**, shown in Figure 1 as $Q_1^{(R)}$.
- **Flow-rate in the left carotid artery**, shown in Figure 1 as $Q_1^{(L)}$.
- **Pressure in the right radial artery**, shown in Figure 1 as $P_3^{(R)}$.
- **Pressure in the left radial artery**, shown in Figure 1 as $P_3^{(L)}$.

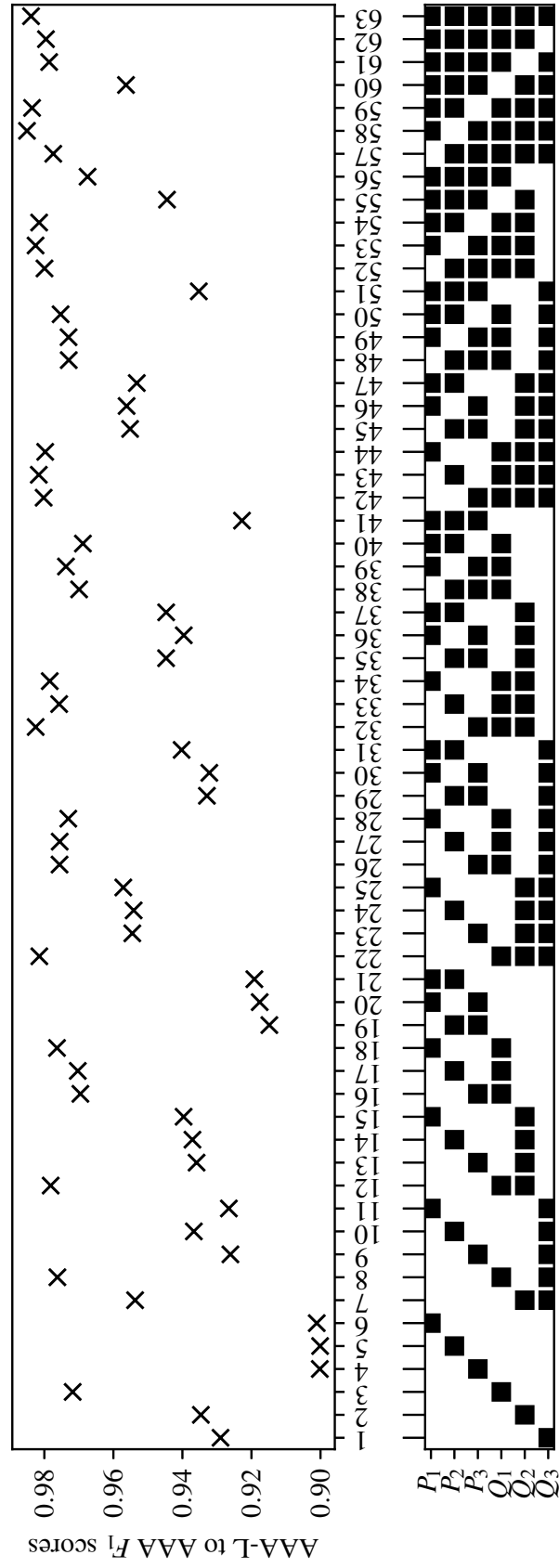


Figure 17: The ratios of the F_1 scores for AAA-L classification relative to AAA classification, when providing each combination of input measurements are shown. Measurements included within each combination are highlighted with a black square.

Carotid artery flow-rate is chosen as it has been shown to be the best measurement for disease classification. Radial artery pressure is chosen due to the location of the radial artery on the human wrist. While wearable devices capable of measuring continuous radial pressure profiles do not currently exist (to the authors’ knowledge), if AAAs can be detected to satisfactory accuracies using these measurements, it may suggest the possibility of future home monitoring of abdominal aortic health through the development of such wearables. The sensitivities and specificities achieved by the four unilateral GB classifiers are shown in Table 11. It shows that relative to the bilateral case, while there is a decrease in the classification accuracies, the magnitude of the decrease is less than 10%. This finding suggests that there may be sufficient biomarkers of AAA presence captured within the intra-measurement details of a single pressure or flow-rate profile. The fact that similar accuracies are achieved with either the right or left instances of any measurement is likely due to physiological symmetry. While there are some minor asymmetries between the right and left upper extremities, due to the topology of the arterial network (as shown in Figure 1) changes to the cross sectional area of the abdominal aorta are expected to produce relatively consistent changes in both the right and left side of the body.

	Side	Sensitivity	Specificity
Carotid flow-rate (Q_1)	Right	0.9369	0.9161
	Left	0.9065	0.9146
	Both	0.9799	0.9811
Radial pressure (P_3)	Right	0.8356	0.8533
	Left	0.8633	0.8605
	Both	0.9202	0.9248

Table 11: The sensitivities and specificities achieved when using the measurements of flow-rate in the right, left, and both CAs and pressure in the right, left, and both radial arteries.

4 Conclusions

The main conclusion of this study is that machine learning methods are suitable for detection of arterial disease—both stenoses and aneurysms—from peripheral measurements of pressure and flow-rates across the network. Amongst various ML methods, it is found that tree-based methods of Random Forest and Gradient Boosting perform best for this application. Across the different forms of disease, the Gradient Boosting method outperforms Random Forest, Support Vector Machine, Naive Bayes, Logistic Regression, and even the deep learning method of Multi-layer Perceptron.

It is demonstrated that maximum F_1 scores larger than 0.9 are achievable for CAS and PAD, larger than 0.85 for SAS, and larger than 0.98 for both low- and high-severity AAAs. The corresponding sensitivities and specificities are also both larger than 90% for CAS and PAD, larger than 85% for SAS, and larger than 98% for both low- and high-severity AAAs. While these maximum scores are for the case when all the six measurements are used, it is also shown that the performance degradation is less than 5% when using only three measurements and less than 10% when using only two measurements, as long as the these measurements are carefully chosen in specific combinations. For the case of AAA, it is further demonstrated that when only a single measurement (either on the left or right side) is used, F_1 scores larger than 0.85 and corresponding sensitivities and specificities larger than 85% are achievable. This aspect encourages the application of AAA monitoring and/or screening through the use of a wearable device. Finally, it is shown through the analysis of several classifiers and feature-importance that, amongst the measurements, the carotid artery flow-rate is a particularly informative measurement to detect the presence of all the four forms of disease considered.

5 Limitations & future work

While the results are encouraging, they are produced on a virtual cohort of subjects. Even though the database is physiologically realistic and carefully constructed, it may be that real patient behaviour differs from those in the VPD. Therefore, future steps should be in applying the trained classifiers here directly to a small cohort of real-patient measurements. The effect of measurement errors and biases is ignored in this study. This aspect can also be considered in future studies, along with relaxing the assumption of mutually exclusive disease. Thus, using either real or virtual databases, classifiers should be built to detect not only the presence of disease, but also identify the type of disease (potentially concomitant disease in multiple locations), its location, and its severity. Further improvements can be also made by further optimising the architectures of the machine and deep learning methods to aim for higher accuracies with fewer, potentially noise- and bias-corrupted, measurements.

Funding

This work is supported by an EPSRC studentship ref. EP/N509553/1 and an EPSRC grant ref. EP/R010811/1.

References

- [1] Fowkes, F. G. R., Rudan, D., Rudan, I., Aboyans, V., Denenberg, J. O., McDermott, M. M., Norman, P. E., Sampson, U. K., Williams, L. J., Mensah, G. A., et al. “Comparison of global estimates of prevalence and risk factors for peripheral artery disease in 2000 and 2010: a systematic review and analysis”. In: *The Lancet* 382.9901 (2013), pp. 1329–1340.
- [2] Shadman, R., Criqui, M. H., Bundens, W. P., Fronek, A., Denenberg, J. O., Gamst, A. C., and McDermott, M. M. “Subclavian artery stenosis: prevalence, risk factors, and association with cardiovascular diseases”. In: *Journal of the American College of Cardiology* 44.3 (2004), pp. 618–623.
- [3] Mathiesen, E. B., Joakimsen, O., and Bønaa, K. H. “Prevalence of and risk factors associated with carotid artery stenosis: the Tromsø Study”. In: *Cerebrovascular diseases* 12.1 (2001), pp. 44–51.
- [4] Li, X., Zhao, G., Zhang, J., Duan, Z., and Xin, S. “Prevalence and trends of the abdominal aortic aneurysms epidemic in general population-a meta-analysis”. In: *PLoS One* 8.12 (2013), e81260.
- [5] Darwood, R., Earnshaw, J. J., Turton, G., Shaw, E., Whyman, M., Poskitt, K., Rodd, C., and Heather, B. “Twenty-year review of abdominal aortic aneurysm screening in men in the county of Gloucestershire, United Kingdom”. In: *Journal of vascular surgery* 56.1 (2012), pp. 8–13.
- [6] Sazonov, I., Khir, A. W., Hacham, W. S., Boileau, E., Carson, J. M., Loon, R. van, Ferguson, C., and Nithiarasu, P. “A novel method for non-invasively detecting the severity and location of aortic aneurysms”. In: *Biomechanics and modeling in mechanobiology* 16.4 (2017), pp. 1225–1242.
- [7] Stergiopulos, N., Young, D., and Rogge, T. “Computer simulation of arterial flow with applications to arterial and aortic stenoses”. In: *Journal of biomechanics* 25.12 (1992), pp. 1477–1488.
- [8] Kononenko, I. “Machine learning for medical diagnosis: history, state of the art and perspective”. In: *Artificial Intelligence in medicine* 23.1 (2001), pp. 89–109.
- [9] Çomak, E., Arslan, A., and Türkoğlu, bibinitperiodI. “A decision support system based on support vector machines for diagnosis of the heart valve diseases”. In: *Computers in biology and Medicine* 37.1 (2007), pp. 21–27.
- [10] Song, M. H., Lee, J., Cho, S. P., Lee, K. J., and Yoo, S. K. “Support vector machine based arrhythmia classification using reduced features”. In: *International Journal of Control, Automation, and Systems* 3.4 (2005), pp. 571–579.
- [11] Khandoker, A. H., Palaniswami, M., and Karmakar, C. K. “Support vector machines for automated recognition of obstructive sleep apnea syndrome from ECG recordings”. In: *IEEE transactions on information technology in biomedicine* 13.1 (2009), pp. 37–48.
- [12] Chakshu, N. K., Sazonov, I., and Nithiarasu, P. “Towards enabling a cardiovascular digital twin for human systemic circulation using inverse analysis”. In: *Biomechanics and Modeling in Mechanobiology* (2020), pp. 1–17.
- [13] Jones, G., Parr, J., Nithiarasu, P., and Pant, S. *A proof of concept study for machine learning application to stenosis detection*. 2021. arXiv: 2102.07614 [cs.LG].
- [14] Jones, G., Parr, J., Nithiarasu, P., and Pant, S. *A physiologically realistic virtual patient database for the study of arterial haemodynamics*. 2021. arXiv: 2102.10655 [physics.med-ph].
- [15] Jones, G., Parr, J., Nithiarasu, P., and Pant, S. “A physiologically realistic virtual patient database for the study of arterial haemodynamics [Data set]”. In: *Zenodo* (Feb. 2021). DOI: 10.5281/zenodo.4549764. URL: <https://doi.org/10.5281/zenodo.4549764>.
- [16] Dyken, M. L., Klatte, E., Kolar, O. J., and Spurgeon, C. “Complete occlusion of common or internal carotid arteries: Clinical significance”. In: *Archives of Neurology* 30.5 (1974), pp. 343–346.
- [17] Kullo, I. J. and Rooke, T. W. “Peripheral artery disease”. In: *New England Journal of Medicine* 374.9 (2016), pp. 861–871.
- [18] Aboyans, V., Desormais, I., Lacroix, P., Salazar, J., Criqui, M. H., and Laskar, M. “The general prognosis of patients with peripheral arterial disease differs according to the disease localization”. In: *Journal of the American College of Cardiology* 55.9 (2010), pp. 898–903.
- [19] Chen, Q., Smith, C. Y., Bailey, K. R., Wennberg, P. W., and Kullo, I. J. “Disease location is associated with survival in patients with peripheral arterial disease”. In: *Journal of the American Heart Association* 2.5 (2013), e000304.

- [20] Subramanian, R., White, C. J., Rosenfield, K., Bashir, R., Almagor, Y., Meerkin, D., and Shalman, E. “Renal fractional flow reserve: a hemodynamic evaluation of moderate renal artery stenoses”. In: *Catheterization and cardiovascular interventions* 64.4 (2005), pp. 480–486.
- [21] Ernst, C. B. “Abdominal aortic aneurysm”. In: *New England Journal of Medicine* 328.16 (1993), pp. 1167–1172.
- [22] Davis, M., Harris, M., and Earnshaw, J. J. “Implementation of the national health service abdominal aortic aneurysm screening program in England”. In: *Journal of vascular surgery* 57.5 (2013), pp. 1440–1445.
- [23] Adji, A., Hirata, K., and O’rourke, M. F. “Clinical use of indices determined non-invasively from the radial and carotid pressure waveforms”. In: *Blood pressure monitoring* 11.4 (2006), pp. 215–221.
- [24] O’rourke, M. F. “Carotid Artery Tonometry: Pros and Cons”. In: *American journal of hypertension* 29.3 (2015), pp. 296–298.
- [25] Guelen, I., Westerhof, B. E., Sar, G. L. van der, Montfrans, G. A. van, Kiemeneij, F., Wesseling, K. H., and Bos, W. J. W. “Validation of brachial artery pressure reconstruction from finger arterial pressure”. In: *Journal of hypertension* 26.7 (2008), pp. 1321–1327.
- [26] Byström, S., Jensen, B., Jensen-Urstad, M., Lindblad, L., and Kilbom, A. “Ultrasound-Doppler technique for monitoring blood flow in the brachial artery compared with occlusion plethysmography of the forearm”. In: *Scandinavian journal of clinical and laboratory investigation* 58.7 (1998), pp. 569–576.
- [27] Oglat, A. A., Matjafri, M., Suardi, N., Oqlat, M. A., Abdelrahman, M. A., and Oqlat, A. A. “A review of medical doppler ultrasonography of blood flow in general and especially in common carotid artery”. In: *Journal of medical ultrasound* 26.1 (2018), p. 3.
- [28] Radegran, G. “Ultrasound Doppler estimates of femoral artery blood flow during dynamic knee extensor exercise in humans”. In: *Journal of Applied Physiology* 83.4 (1997), pp. 1383–1388.
- [29] Mohamad, I. B. and Usman, D. “Standardization and its effects on K-means clustering algorithm”. In: *Research Journal of Applied Sciences, Engineering and Technology* 6.17 (2013), pp. 3299–3303.
- [30] Liaw, A., Wiener, M., et al. “Classification and regression by randomForest”. In: *R news* 2.3 (2002), pp. 18–22.
- [31] Breiman, L. “Random forests”. In: *Machine learning* 45.1 (2001), pp. 5–32.
- [32] Friedman, J. H. “Greedy function approximation: a gradient boosting machine”. In: *Annals of statistics* (2001), pp. 1189–1232.
- [33] Elith, J., Leathwick, J. R., and Hastie, T. “A working guide to boosted regression trees”. In: *Journal of Animal Ecology* 77.4 (2008), pp. 802–813.
- [34] Rish, I. et al. “An empirical study of the naive Bayes classifier”. In: *IJCAI 2001 workshop on empirical methods in artificial intelligence*. Vol. 3. 22. 2001, pp. 41–46.
- [35] Rish, I., Hellerstein, J., and Thathachar, J. “An analysis of data characteristics that affect naive Bayes performance”. In: *IBM TJ Watson Research Center* 30 (2001), pp. 1–8.
- [36] Kecman, V. “Support vector machines—an introduction”. In: *Support vector machines: theory and applications*. Springer, 2005, pp. 1–47.
- [37] Sperandei, S. “Understanding logistic regression analysis”. In: *Biochemia medica: Biochemia medica* 24.1 (2014), pp. 12–18.
- [38] Hilbe, J. M. *Logistic regression models*. CRC press, 2009.
- [39] Murtagh, F. “Multilayer perceptrons for classification and regression”. In: *Neurocomputing* 2.5-6 (1991), pp. 183–197.
- [40] Pedregosa, F., Varoquaux, G., Gramfort, A., Michel, V., Thirion, B., Grisel, O., Blondel, M., Prettenhofer, P., Weiss, R., Dubourg, V., et al. “Scikit-learn: Machine learning in Python”. In: *the Journal of machine Learning research* 12 (2011), pp. 2825–2830.
- [41] Jakkula, V. “Tutorial on support vector machine (svm)”. In: *School of EECS, Washington State University* 37 (2006).
- [42] Scholkopf, B., Sung, K.-K., Burges, C. J., Girosi, F., Niyogi, P., Poggio, T., and Vapnik, V. “Comparing support vector machines with Gaussian kernels to radial basis function classifiers”. In: *IEEE transactions on Signal Processing* 45.11 (1997), pp. 2758–2765.
- [43] Murphy, K. P. et al. “Naive bayes classifiers”. In: *University of British Columbia* 18.60 (2006).
- [44] Hastie, T., Tibshirani, R., and Friedman, J. *The elements of statistical learning: data mining, inference, and prediction*. Springer Science & Business Media, 2009.

- [45] Low, K, Loon, R van, Sazonov, I, Bevan, R., and Nithiarasu, P. “An improved baseline model for a human arterial network to study the impact of aneurysms on pressure-flow waveforms”. In: *International journal for numerical methods in biomedical engineering* 28.12 (2012), pp. 1224–1246.
- [46] Zhou, Z. and Hooker, G. *Unbiased Measurement of Feature Importance in Tree-Based Methods*. 2020. arXiv: 1903.05179 [stat.ML].

A CAS combination search results

The F_1 scores, sensitivities, and specificities achieved for CAS classification when using each of the six ML methods are shown in Table 12, 13, and 14 respectively.

Input combination	Classification method					
	NB	LR	SVM	RF	MLP	GB
Q_3	0.5547	0.5110	0.5157	0.5807	0.4365	0.5606
Q_2	0.5105	0.5080	0.4955	0.6858	0.4410	0.6565
Q_1	0.5676	0.5033	0.5953	0.8809	0.6459	0.8521
P_3	0.4927	0.5023	0.4991	0.5441	0.4805	0.5131
P_2	0.4413	0.5066	0.5260	0.5628	0.3741	0.5412
P_1	0.5473	0.4917	0.5712	0.6681	0.7013	0.7082
Q_3, Q_2	0.5684	0.4955	0.5104	0.6955	0.4915	0.6889
Q_3, Q_1	0.4831	0.5050	0.5544	0.8790	0.6944	0.8629
Q_3, P_3	0.5213	0.4935	0.5124	0.5825	0.4929	0.5659
Q_3, P_2	0.5853	0.5018	0.5142	0.5918	0.4904	0.5849
Q_3, P_1	0.5048	0.5034	0.5576	0.6601	0.6864	0.7105
Q_2, Q_1	0.4600	0.4975	0.5540	0.8913	0.6648	0.8824
Q_2, P_3	0.4804	0.4940	0.5109	0.6833	0.4158	0.6805
Q_2, P_2	0.5290	0.5037	0.5125	0.6836	0.5618	0.6908
Q_2, P_1	0.4434	0.4978	0.5597	0.7204	0.6741	0.7562
Q_1, P_3	0.4470	0.4990	0.5595	0.8732	0.6860	0.8577
Q_1, P_2	0.5341	0.5029	0.5629	0.8774	0.7090	0.8684
Q_1, P_1	0.4927	0.5018	0.6233	0.8837	0.7822	0.8850
P_3, P_2	0.5507	0.5117	0.5263	0.5581	0.5313	0.5431
P_3, P_1	0.5266	0.4963	0.5725	0.6837	0.7384	0.7539
P_2, P_1	0.5089	0.4944	0.6885	0.7938	0.8878	0.8950
Q_3, Q_2, Q_1	0.4299	0.4995	0.5425	0.8907	0.6838	0.8868
Q_3, Q_2, P_3	0.4822	0.4980	0.5058	0.6910	0.5300	0.7072
Q_3, Q_2, P_2	0.5346	0.4975	0.5204	0.6962	0.5211	0.7102
Q_3, Q_2, P_1	0.5267	0.5024	0.5428	0.7229	0.6084	0.7693
Q_3, Q_1, P_3	0.4636	0.5016	0.5317	0.8685	0.6699	0.8660
Q_3, Q_1, P_2	0.5186	0.4960	0.5580	0.8751	0.6469	0.8728
Q_3, Q_1, P_1	0.5257	0.5020	0.5888	0.8843	0.7532	0.8903
Q_3, P_3, P_2	0.4493	0.5032	0.5119	0.5923	0.5418	0.5888
Q_3, P_3, P_1	0.5019	0.4892	0.5527	0.6751	0.7159	0.7602
Q_3, P_2, P_1	0.4312	0.5042	0.6303	0.7564	0.8623	0.8923
Q_2, Q_1, P_3	0.5222	0.5041	0.5300	0.8840	0.6354	0.8776
Q_2, Q_1, P_2	0.5155	0.4957	0.5586	0.8847	0.7001	0.8844
Q_2, Q_1, P_1	0.5251	0.4940	0.6039	0.8941	0.7611	0.8968
Q_2, P_3, P_2	0.4893	0.5041	0.5241	0.6824	0.5335	0.6929
Q_2, P_3, P_1	0.4067	0.4965	0.5421	0.7249	0.7185	0.8064
Q_2, P_2, P_1	0.5479	0.4858	0.6415	0.7740	0.8735	0.9040
Q_1, P_3, P_2	0.4766	0.4969	0.5505	0.8700	0.7048	0.8651
Q_1, P_3, P_1	0.5037	0.4908	0.5975	0.8777	0.7645	0.8956
Q_1, P_2, P_1	0.4997	0.4972	0.6772	0.8872	0.8680	0.9389
P_3, P_2, P_1	0.5090	0.4997	0.6451	0.7694	0.8831	0.8936
Q_3, Q_2, Q_1, P_3	0.4569	0.4921	0.5408	0.8835	0.6258	0.8855
Q_3, Q_2, Q_1, P_2	0.4253	0.5022	0.5462	0.8871	0.6655	0.8887
Q_3, Q_2, Q_1, P_1	0.4934	0.5068	0.5783	0.8925	0.7163	0.9004
Q_3, Q_2, P_3, P_2	0.4875	0.5026	0.5234	0.6852	0.5483	0.7145
Q_3, Q_2, P_3, P_1	0.4481	0.4945	0.5399	0.7231	0.6714	0.8125
Q_3, Q_2, P_2, P_1	0.4329	0.5034	0.6043	0.7619	0.8618	0.9025
Q_3, Q_1, P_3, P_2	0.4934	0.4972	0.5400	0.8717	0.6299	0.8761
Q_3, Q_1, P_3, P_1	0.5365	0.5011	0.5802	0.8789	0.7197	0.8978
Q_3, Q_1, P_2, P_1	0.5068	0.4974	0.6338	0.8852	0.8542	0.9395
Q_3, P_3, P_2, P_1	0.4329	0.4980	0.6137	0.7393	0.8471	0.8906
Q_2, Q_1, P_3, P_2	0.5669	0.4933	0.5468	0.8822	0.6524	0.8844
Q_2, Q_1, P_3, P_1	0.5193	0.4978	0.5783	0.8878	0.7207	0.9065
Q_2, Q_1, P_2, P_1	0.4638	0.5037	0.6413	0.8944	0.8683	0.9383
Q_2, P_3, P_2, P_1	0.4868	0.4999	0.6142	0.7694	0.8503	0.9084
Q_1, P_3, P_2, P_1	0.4735	0.5025	0.6320	0.8807	0.8547	0.9353
Q_3, Q_2, Q_1, P_3, P_2	0.5005	0.5015	0.5387	0.8848	0.6322	0.8927
Q_3, Q_2, Q_1, P_3, P_1	0.4652	0.4962	0.5760	0.8875	0.7079	0.9093
Q_3, Q_2, Q_1, P_2, P_1	0.5108	0.4994	0.6088	0.8934	0.8313	0.9381
Q_3, Q_2, P_3, P_2, P_1	0.4994	0.5105	0.5808	0.7540	0.8463	0.9052
Q_3, Q_1, P_3, P_2, P_1	0.5330	0.5024	0.6108	0.8849	0.8380	0.9364
Q_2, Q_1, P_3, P_2, P_1	0.4899	0.5054	0.6026	0.8900	0.8371	0.9391
$Q_3, Q_2, Q_1, P_3, P_2, P_1$	0.4634	0.5018	0.5862	0.8878	0.7785	0.9343

Table 12: The F_1 scores achieved across the combination search by each of the six classification methods.

Input combination	Classification method					
	NB	LR	SVM	RF	MLP	GB
Q_3	0.1531	0.5527	0.4283	0.5572	0.6084	0.5736
Q_2	0.6641	0.5097	0.6418	0.6575	0.6228	0.6744
Q_1	0.5426	0.4525	0.5694	0.8704	0.4243	0.8547
P_3	0.5024	0.5098	0.4999	0.5139	0.5355	0.5158
P_2	0.6490	0.4979	0.5052	0.5366	0.7038	0.5491
P_1	0.2410	0.4992	0.6588	0.6510	0.7052	0.7215
Q_3, Q_2	0.5055	0.5035	0.5651	0.6655	0.5439	0.7044
Q_3, Q_1	0.7217	0.5094	0.5461	0.8681	0.6288	0.8661
Q_3, P_3	0.4462	0.5091	0.4944	0.5615	0.5226	0.5583
Q_3, P_2	0.3652	0.5090	0.5111	0.5731	0.5572	0.5777
Q_3, P_1	0.3032	0.5049	0.6510	0.6411	0.7334	0.7149
Q_2, Q_1	0.4543	0.5091	0.5770	0.8765	0.6372	0.8845
Q_2, P_3	0.5395	0.5117	0.5263	0.6555	0.6691	0.6926
Q_2, P_2	0.6043	0.4987	0.5436	0.6563	0.3867	0.7117
Q_2, P_1	0.5766	0.4905	0.6442	0.6962	0.6879	0.7668
Q_1, P_3	0.4718	0.5003	0.5461	0.8679	0.7167	0.8601
Q_1, P_2	0.3903	0.5068	0.5438	0.8672	0.7467	0.8664
Q_1, P_1	0.6488	0.4978	0.6672	0.8798	0.8290	0.8848
P_3, P_2	0.4744	0.5034	0.5251	0.5383	0.4863	0.5335
P_3, P_1	0.3334	0.4815	0.6303	0.6599	0.7469	0.7842
P_2, P_1	0.4943	0.5001	0.6699	0.7762	0.8995	0.9026
Q_3, Q_2, Q_1	0.4935	0.4812	0.5598	0.8789	0.6425	0.8896
Q_3, Q_2, P_3	0.5586	0.4913	0.5454	0.6647	0.5014	0.7219
Q_3, Q_2, P_2	0.4348	0.5091	0.5336	0.6788	0.5298	0.7313
Q_3, Q_2, P_1	0.2964	0.5165	0.6068	0.6975	0.6471	0.7783
Q_3, Q_1, P_3	0.4427	0.5021	0.5321	0.8620	0.6388	0.8677
Q_3, Q_1, P_2	0.4268	0.4974	0.5605	0.8718	0.6645	0.8721
Q_3, Q_1, P_1	0.5134	0.4687	0.6341	0.8735	0.7474	0.8936
Q_3, P_3, P_2	0.6823	0.4939	0.5076	0.5698	0.4853	0.5905
Q_3, P_3, P_1	0.3887	0.4941	0.5882	0.6691	0.6907	0.7866
Q_3, P_2, P_1	0.6288	0.4919	0.6251	0.7473	0.8593	0.8928
Q_2, Q_1, P_3	0.4599	0.5056	0.5474	0.8735	0.6999	0.8819
Q_2, Q_1, P_2	0.4296	0.5085	0.5728	0.8766	0.6703	0.8853
Q_2, Q_1, P_1	0.5235	0.5037	0.6393	0.8825	0.7635	0.8991
Q_2, P_3, P_2	0.3581	0.4902	0.5484	0.6566	0.5249	0.7098
Q_2, P_3, P_1	0.6042	0.4816	0.6079	0.7001	0.7140	0.8277
Q_2, P_2, P_1	0.5758	0.4826	0.6481	0.7516	0.8780	0.9114
Q_1, P_3, P_2	0.4530	0.4984	0.5521	0.8616	0.6733	0.8651
Q_1, P_3, P_1	0.4760	0.4859	0.6233	0.8721	0.7403	0.8993
Q_1, P_2, P_1	0.4610	0.4917	0.6744	0.8807	0.8797	0.9433
P_3, P_2, P_1	0.4001	0.5159	0.6442	0.7562	0.8731	0.8930
Q_3, Q_2, Q_1, P_3	0.5792	0.4903	0.5548	0.8700	0.6711	0.8916
Q_3, Q_2, Q_1, P_2	0.6211	0.4961	0.5726	0.8788	0.6622	0.8933
Q_3, Q_2, Q_1, P_1	0.5018	0.4831	0.5948	0.8837	0.7442	0.9015
Q_3, Q_2, P_3, P_2	0.5499	0.4981	0.4938	0.6722	0.4844	0.7277
Q_3, Q_2, P_3, P_1	0.4381	0.5052	0.5948	0.7055	0.6997	0.8337
Q_3, Q_2, P_2, P_1	0.7010	0.5049	0.6401	0.7463	0.8600	0.9129
Q_3, Q_1, P_3, P_2	0.4629	0.5000	0.5424	0.8597	0.6331	0.8747
Q_3, Q_1, P_3, P_1	0.4436	0.4937	0.6099	0.8747	0.7555	0.9017
Q_3, Q_1, P_2, P_1	0.5362	0.5062	0.6300	0.8761	0.8538	0.9417
Q_3, P_3, P_2, P_1	0.6073	0.5011	0.6165	0.7243	0.8391	0.8993
Q_2, Q_1, P_3, P_2	0.4973	0.5056	0.5779	0.8729	0.6427	0.8874
Q_2, Q_1, P_3, P_1	0.4225	0.5065	0.6115	0.8813	0.7596	0.9100
Q_2, Q_1, P_2, P_1	0.5115	0.4954	0.6345	0.8858	0.8618	0.9416
Q_2, P_3, P_2, P_1	0.5582	0.4877	0.6266	0.7498	0.8573	0.9133
Q_1, P_3, P_2, P_1	0.5769	0.4891	0.6309	0.8674	0.8667	0.9375
Q_3, Q_2, Q_1, P_3, P_2	0.5446	0.4929	0.5686	0.8759	0.6487	0.8949
Q_3, Q_2, Q_1, P_3, P_1	0.4676	0.4933	0.6021	0.8775	0.7169	0.9117
Q_3, Q_2, Q_1, P_2, P_1	0.5403	0.5015	0.6142	0.8858	0.8288	0.9415
Q_3, Q_2, P_3, P_2, P_1	0.6396	0.5042	0.6070	0.7375	0.8308	0.9120
Q_3, Q_1, P_3, P_2, P_1	0.5330	0.4920	0.6171	0.8795	0.8345	0.9399
Q_2, Q_1, P_3, P_2, P_1	0.4640	0.4919	0.6149	0.8774	0.8273	0.9416
$Q_3, Q_2, Q_1, P_3, P_2, P_1$	0.6224	0.5116	0.6012	0.8747	0.7916	0.9364

Table 13: The sensitivities achieved across the combination search by each of the six classification methods.

Input combination	Classification method					
	NB	LR	SVM	RF	MLP	GB
Q_3	0.7090	0.4968	0.5462	0.5904	0.3886	0.5556
Q_2	0.4579	0.5075	0.4474	0.7006	0.3896	0.6479
Q_1	0.5776	0.5204	0.6063	0.8893	0.7517	0.8502
P_3	0.4896	0.4998	0.4989	0.5555	0.4632	0.5122
P_2	0.3826	0.5096	0.5335	0.5732	0.2983	0.5384
P_1	0.6628	0.4893	0.5363	0.6767	0.6993	0.7010
Q_3, Q_2	0.5935	0.4929	0.4917	0.7116	0.4745	0.6808
Q_3, Q_1	0.4072	0.5036	0.5576	0.8876	0.7293	0.8605
Q_3, P_3	0.5478	0.4884	0.5187	0.5912	0.4832	0.5690
Q_3, P_2	0.6764	0.4995	0.5153	0.5998	0.4687	0.5879
Q_3, P_1	0.5730	0.5030	0.5215	0.6696	0.6619	0.7081
Q_2, Q_1	0.4618	0.4937	0.5453	0.9032	0.6786	0.8808
Q_2, P_3	0.4618	0.4883	0.5057	0.6978	0.3494	0.6743
Q_2, P_2	0.5020	0.5055	0.5018	0.6978	0.6303	0.6798
Q_2, P_1	0.4055	0.5003	0.5269	0.7341	0.6672	0.7498
Q_1, P_3	0.4399	0.4987	0.5648	0.8774	0.6701	0.8560
Q_1, P_2	0.5865	0.5016	0.5704	0.8855	0.6883	0.8701
Q_1, P_1	0.4417	0.5032	0.6035	0.8869	0.7522	0.8853
P_3, P_2	0.5798	0.5146	0.5268	0.5659	0.5477	0.5467
P_3, P_1	0.5958	0.5013	0.5494	0.6961	0.7335	0.7356
P_2, P_1	0.5140	0.4926	0.6983	0.8054	0.8785	0.8889
Q_3, Q_2, Q_1	0.4125	0.5057	0.5361	0.9002	0.7054	0.8846
Q_3, Q_2, P_3	0.4580	0.5003	0.4925	0.7049	0.5404	0.6992
Q_3, Q_2, P_2	0.5711	0.4937	0.5158	0.7055	0.5181	0.6986
Q_3, Q_2, P_1	0.6091	0.4977	0.5190	0.7374	0.5915	0.7638
Q_3, Q_1, P_3	0.4700	0.5015	0.5316	0.8735	0.6857	0.8648
Q_3, Q_1, P_2	0.5508	0.4956	0.5571	0.8777	0.6386	0.8734
Q_3, Q_1, P_1	0.5302	0.5132	0.5699	0.8929	0.7568	0.8877
Q_3, P_3, P_2	0.3818	0.5064	0.5135	0.6018	0.5629	0.5882
Q_3, P_3, P_1	0.5399	0.4877	0.5392	0.6782	0.7300	0.7441
Q_3, P_2, P_1	0.3769	0.5084	0.6328	0.7620	0.8646	0.8920
Q_2, Q_1, P_3	0.5443	0.5037	0.5238	0.8924	0.6055	0.8743
Q_2, Q_1, P_2	0.5454	0.4916	0.5531	0.8913	0.7162	0.8838
Q_2, Q_1, P_1	0.5258	0.4909	0.5886	0.9035	0.7597	0.8950
Q_2, P_3, P_2	0.5319	0.5088	0.5156	0.6959	0.5367	0.6840
Q_2, P_3, P_1	0.3563	0.5015	0.5177	0.7390	0.7211	0.7921
Q_2, P_2, P_1	0.5374	0.4869	0.6385	0.7882	0.8701	0.8979
Q_1, P_3, P_2	0.4840	0.4965	0.5500	0.8766	0.7220	0.8651
Q_1, P_3, P_1	0.5131	0.4924	0.5866	0.8822	0.7795	0.8927
Q_1, P_2, P_1	0.5126	0.4991	0.6787	0.8925	0.8592	0.9351
P_3, P_2, P_1	0.5462	0.4944	0.6456	0.7777	0.8911	0.8942
Q_3, Q_2, Q_1, P_3	0.4208	0.4928	0.5357	0.8943	0.6053	0.8807
Q_3, Q_2, Q_1, P_2	0.3725	0.5043	0.5363	0.8938	0.6672	0.8852
Q_3, Q_2, Q_1, P_1	0.4907	0.5149	0.5716	0.8996	0.7008	0.8995
Q_3, Q_2, P_3, P_2	0.4675	0.5042	0.5340	0.6921	0.5725	0.7072
Q_3, Q_2, P_3, P_1	0.4510	0.4911	0.5196	0.7331	0.6572	0.7981
Q_3, Q_2, P_2, P_1	0.3589	0.5029	0.5888	0.7716	0.8632	0.8941
Q_3, Q_1, P_3, P_2	0.5034	0.4963	0.5392	0.8811	0.6285	0.8773
Q_3, Q_1, P_3, P_1	0.5706	0.5037	0.5681	0.8823	0.6997	0.8947
Q_3, Q_1, P_2, P_1	0.4969	0.4946	0.6357	0.8926	0.8545	0.9376
Q_3, P_3, P_2, P_1	0.3848	0.4970	0.6126	0.7481	0.8530	0.8837
Q_2, Q_1, P_3, P_2	0.5945	0.4893	0.5352	0.8896	0.6571	0.8822
Q_2, Q_1, P_3, P_1	0.5533	0.4950	0.5648	0.8930	0.6989	0.9037
Q_2, Q_1, P_2, P_1	0.4495	0.5065	0.6446	0.9015	0.8734	0.9355
Q_2, P_3, P_2, P_1	0.4639	0.5040	0.6088	0.7818	0.8452	0.9045
Q_1, P_3, P_2, P_1	0.4415	0.5070	0.6326	0.8912	0.8458	0.9335
Q_3, Q_2, Q_1, P_3, P_2	0.4859	0.5044	0.5277	0.8919	0.6246	0.8911
Q_3, Q_2, Q_1, P_3, P_1	0.4646	0.4972	0.5655	0.8956	0.7031	0.9073
Q_3, Q_2, Q_1, P_2, P_1	0.5008	0.4988	0.6065	0.8996	0.8332	0.9351
Q_3, Q_2, P_3, P_2, P_1	0.4528	0.5127	0.5701	0.7641	0.8577	0.8996
Q_3, Q_1, P_3, P_2, P_1	0.5331	0.5060	0.6081	0.8892	0.8406	0.9334
Q_2, Q_1, P_3, P_2, P_1	0.4984	0.5101	0.5974	0.9002	0.8442	0.9370
$Q_3, Q_2, Q_1, P_3, P_2, P_1$	0.4155	0.4986	0.5800	0.8984	0.7703	0.9325

Table 14: The specificities achieved across the combination search by each of the six classification methods.

B SAS combination search results

The F_1 scores, sensitivities, and specificities achieved for SAS classification when using each of the six ML methods are shown in Table 15, 16, and 17 respectively.

Input combination	Classification method					
	NB	LR	SVM	RF	MLP	GB
Q_3	0.5041	0.5288	0.4897	0.5723	0.5403	0.5592
Q_2	0.4681	0.5004	0.4839	0.7577	0.5691	0.7415
Q_1	0.3799	0.5028	0.4923	0.7779	0.6176	0.7529
P_3	0.4931	0.4972	0.5097	0.5530	0.5474	0.5331
P_2	0.4698	0.4990	0.5528	0.5627	0.4895	0.5453
P_1	0.5344	0.5023	0.5035	0.5171	0.5571	0.5060
Q_3, Q_2	0.4529	0.5136	0.5075	0.7623	0.4939	0.7608
Q_3, Q_1	0.4588	0.4893	0.5053	0.7814	0.5414	0.7758
Q_3, P_3	0.4992	0.4963	0.5207	0.5824	0.5463	0.5746
Q_3, P_2	0.5497	0.5068	0.5306	0.5869	0.5215	0.5850
Q_3, P_1	0.4195	0.5099	0.4992	0.5685	0.4776	0.5627
Q_2, Q_1	0.5064	0.5010	0.5025	0.8450	0.5853	0.8461
Q_2, P_3	0.4818	0.5020	0.5294	0.7555	0.6054	0.7694
Q_2, P_2	0.5116	0.5020	0.5405	0.7586	0.5454	0.7711
Q_2, P_1	0.5468	0.4913	0.5353	0.7568	0.5124	0.7609
Q_1, P_3	0.4564	0.4963	0.5252	0.7697	0.5067	0.7522
Q_1, P_2	0.5209	0.4986	0.5388	0.7708	0.5833	0.7606
Q_1, P_1	0.5186	0.5005	0.5327	0.7744	0.5426	0.7751
P_3, P_2	0.5450	0.5031	0.5256	0.5695	0.4960	0.5626
P_3, P_1	0.5464	0.4996	0.5282	0.5450	0.5510	0.5338
P_2, P_1	0.5399	0.5041	0.5447	0.5669	0.5133	0.5766
Q_3, Q_2, Q_1	0.4574	0.5081	0.5284	0.8447	0.5866	0.8552
Q_3, Q_2, P_3	0.5499	0.4925	0.5254	0.7624	0.5847	0.7830
Q_3, Q_2, P_2	0.4591	0.4936	0.5272	0.7629	0.5742	0.7829
Q_3, Q_2, P_1	0.4240	0.4980	0.5099	0.7627	0.4969	0.7800
Q_3, Q_1, P_3	0.4810	0.4994	0.5173	0.7808	0.5511	0.7691
Q_3, Q_1, P_2	0.4098	0.5069	0.5354	0.7749	0.5611	0.7750
Q_3, Q_1, P_1	0.5414	0.4999	0.5095	0.7761	0.5230	0.7880
Q_3, P_3, P_2	0.4492	0.5021	0.5330	0.5892	0.5636	0.5900
Q_3, P_3, P_1	0.4912	0.4971	0.5248	0.5767	0.5253	0.5759
Q_3, P_2, P_1	0.4476	0.4914	0.5259	0.5883	0.5758	0.5961
Q_2, Q_1, P_3	0.5243	0.5008	0.5154	0.8381	0.5874	0.8427
Q_2, Q_1, P_2	0.4994	0.5029	0.5349	0.8402	0.6139	0.8469
Q_2, Q_1, P_1	0.4988	0.5042	0.5279	0.8413	0.5861	0.8492
Q_2, P_3, P_2	0.5272	0.4992	0.5284	0.7549	0.5760	0.7802
Q_2, P_3, P_1	0.4351	0.5048	0.5351	0.7479	0.5724	0.7726
Q_2, P_2, P_1	0.5318	0.5081	0.5316	0.7563	0.5258	0.7752
Q_1, P_3, P_2	0.5152	0.5030	0.5454	0.7624	0.5782	0.7579
Q_1, P_3, P_1	0.4607	0.5022	0.5235	0.7690	0.5069	0.7680
Q_1, P_2, P_1	0.5437	0.5019	0.5319	0.7670	0.5930	0.7733
P_3, P_2, P_1	0.5314	0.4984	0.5352	0.5661	0.5518	0.5826
Q_3, Q_2, Q_1, P_3	0.4910	0.4925	0.5169	0.8407	0.5706	0.8541
Q_3, Q_2, Q_1, P_2	0.5113	0.5036	0.5301	0.8432	0.5952	0.8585
Q_3, Q_2, Q_1, P_1	0.5097	0.5078	0.5191	0.8404	0.5828	0.8558
Q_3, Q_2, P_3, P_2	0.4738	0.4968	0.5206	0.7549	0.5628	0.7879
Q_3, Q_2, P_3, P_1	0.4721	0.4944	0.5224	0.7545	0.5605	0.7857
Q_3, Q_2, P_2, P_1	0.5592	0.5081	0.5331	0.7616	0.5854	0.7911
Q_3, Q_1, P_3, P_2	0.4762	0.4987	0.5259	0.7738	0.5791	0.7711
Q_3, Q_1, P_3, P_1	0.4558	0.5108	0.5339	0.7749	0.5766	0.7850
Q_3, Q_1, P_2, P_1	0.4066	0.4957	0.5279	0.7719	0.5785	0.7813
Q_3, P_3, P_2, P_1	0.5257	0.4878	0.5395	0.5866	0.5695	0.5988
Q_2, Q_1, P_3, P_2	0.5318	0.4975	0.5487	0.8357	0.6064	0.8488
Q_2, Q_1, P_3, P_1	0.5348	0.4987	0.5326	0.8350	0.5879	0.8516
Q_2, Q_1, P_2, P_1	0.5537	0.5113	0.5337	0.8362	0.6258	0.8545
Q_2, P_3, P_2, P_1	0.4863	0.4966	0.5394	0.7458	0.6102	0.7797
Q_1, P_3, P_2, P_1	0.4711	0.5010	0.5358	0.7635	0.6088	0.7738
Q_3, Q_2, Q_1, P_3, P_2	0.4763	0.5038	0.5312	0.8330	0.5966	0.8534
Q_3, Q_2, Q_1, P_3, P_1	0.4953	0.4998	0.5212	0.8399	0.5809	0.8571
Q_3, Q_2, Q_1, P_2, P_1	0.4917	0.5099	0.5304	0.8390	0.6070	0.8600
Q_3, Q_2, P_3, P_2, P_1	0.5344	0.5069	0.5292	0.7540	0.5963	0.7913
Q_3, Q_1, P_3, P_2, P_1	0.5205	0.4991	0.5309	0.7734	0.5740	0.7828
Q_2, Q_1, P_3, P_2, P_1	0.4912	0.5012	0.5353	0.8325	0.6302	0.8502
$Q_3, Q_2, Q_1, P_3, P_2, P_1$	0.4642	0.5016	0.5301	0.8292	0.6040	0.8574

Table 15: The F_1 scores achieved across the combination search by each of the six classification methods.

Input combination	Classification method					
	NB	LR	SVM	RF	MLP	GB
Q_3	0.2997	0.4576	0.5129	0.5678	0.4059	0.5585
Q_2	0.5460	0.5348	0.6918	0.7517	0.3839	0.7366
Q_1	0.7074	0.4613	0.6338	0.7582	0.1873	0.7224
P_3	0.4402	0.5127	0.5616	0.5453	0.3978	0.5431
P_2	0.5140	0.4981	0.4783	0.5629	0.5704	0.5717
P_1	0.4446	0.4836	0.4741	0.5177	0.3803	0.5244
Q_3, Q_2	0.5683	0.4928	0.5411	0.7612	0.5901	0.7585
Q_3, Q_1	0.4887	0.4947	0.5036	0.7630	0.4709	0.7504
Q_3, P_3	0.6479	0.5019	0.5147	0.5720	0.4578	0.5808
Q_3, P_2	0.5719	0.4985	0.5163	0.5849	0.5223	0.5999
Q_3, P_1	0.6081	0.4947	0.4958	0.5633	0.5570	0.5788
Q_2, Q_1	0.6572	0.5008	0.6082	0.8374	0.4909	0.8293
Q_2, P_3	0.5785	0.4860	0.5626	0.7505	0.4320	0.7710
Q_2, P_2	0.4241	0.4801	0.5294	0.7560	0.6660	0.7763
Q_2, P_1	0.2405	0.5006	0.5127	0.7500	0.5838	0.7601
Q_1, P_3	0.5330	0.4970	0.5596	0.7534	0.5809	0.7305
Q_1, P_2	0.4943	0.5180	0.5282	0.7545	0.4884	0.7434
Q_1, P_1	0.5761	0.4991	0.5430	0.7516	0.6004	0.7549
P_3, P_2	0.4714	0.4939	0.5388	0.5668	0.6677	0.5744
P_3, P_1	0.5408	0.4954	0.5252	0.5406	0.4456	0.5421
P_2, P_1	0.4115	0.4958	0.4761	0.5761	0.6175	0.6056
Q_3, Q_2, Q_1	0.5695	0.5019	0.5106	0.8271	0.5303	0.8453
Q_3, Q_2, P_3	0.5651	0.5115	0.5075	0.7621	0.5044	0.7826
Q_3, Q_2, P_2	0.5768	0.5219	0.5101	0.7590	0.5941	0.7882
Q_3, Q_2, P_1	0.6416	0.5013	0.5350	0.7494	0.5963	0.7766
Q_3, Q_1, P_3	0.4649	0.5074	0.5237	0.7550	0.5783	0.7491
Q_3, Q_1, P_2	0.6031	0.50	0.5056	0.7584	0.5796	0.7514
Q_3, Q_1, P_1	0.3262	0.4942	0.5535	0.7527	0.6028	0.7677
Q_3, P_3, P_2	0.5316	0.4904	0.5184	0.5924	0.4985	0.6109
Q_3, P_3, P_1	0.3543	0.4949	0.5116	0.5765	0.5444	0.5855
Q_3, P_2, P_1	0.5225	0.5038	0.5041	0.5864	0.5018	0.6186
Q_2, Q_1, P_3	0.4531	0.4826	0.5427	0.8186	0.6309	0.8303
Q_2, Q_1, P_2	0.4642	0.5029	0.5481	0.8277	0.6178	0.8312
Q_2, Q_1, P_1	0.5179	0.5049	0.5544	0.8268	0.5788	0.8388
Q_2, P_3, P_2	0.5155	0.4806	0.5642	0.7500	0.6050	0.7757
Q_2, P_3, P_1	0.6119	0.4972	0.5365	0.7486	0.5358	0.7752
Q_2, P_2, P_1	0.5590	0.5214	0.5403	0.7578	0.7119	0.7791
Q_1, P_3, P_2	0.4890	0.5159	0.5345	0.7414	0.5886	0.7437
Q_1, P_3, P_1	0.5256	0.5041	0.5548	0.7498	0.6421	0.7479
Q_1, P_2, P_1	0.4038	0.5014	0.5175	0.7490	0.5995	0.7621
P_3, P_2, P_1	0.4461	0.4995	0.5216	0.5697	0.6360	0.6026
Q_3, Q_2, Q_1, P_3	0.6262	0.5155	0.5310	0.8274	0.6144	0.8411
Q_3, Q_2, Q_1, P_2	0.4646	0.5158	0.5531	0.8303	0.6113	0.8487
Q_3, Q_2, Q_1, P_1	0.4913	0.5011	0.5522	0.8242	0.5723	0.8466
Q_3, Q_2, P_3, P_2	0.5435	0.4831	0.54	0.7566	0.64	0.7924
Q_3, Q_2, P_3, P_1	0.5466	0.4884	0.5173	0.7534	0.5521	0.7874
Q_3, Q_2, P_2, P_1	0.4776	0.5022	0.5413	0.7555	0.5892	0.7900
Q_3, Q_1, P_3, P_2	0.5274	0.5010	0.5377	0.7587	0.5758	0.7545
Q_3, Q_1, P_3, P_1	0.4177	0.4823	0.5051	0.7560	0.5163	0.7675
Q_3, Q_1, P_2, P_1	0.5806	0.5103	0.5087	0.7550	0.5940	0.7735
Q_3, P_3, P_2, P_1	0.46	0.5052	0.5204	0.5857	0.6047	0.6121
Q_2, Q_1, P_3, P_2	0.4529	0.5117	0.5461	0.8241	0.6431	0.8413
Q_2, Q_1, P_3, P_1	0.2714	0.4964	0.5150	0.8186	0.6153	0.8437
Q_2, Q_1, P_2, P_1	0.5132	0.5057	0.5357	0.8214	0.6157	0.8386
Q_2, P_3, P_2, P_1	0.4464	0.5042	0.5606	0.7407	0.6294	0.7833
Q_1, P_3, P_2, P_1	0.4715	0.5032	0.5476	0.7439	0.6014	0.7599
Q_3, Q_2, Q_1, P_3, P_2	0.44	0.4889	0.5266	0.8175	0.5881	0.8510
Q_3, Q_2, Q_1, P_3, P_1	0.3896	0.4988	0.5447	0.8256	0.6080	0.8443
Q_3, Q_2, Q_1, P_2, P_1	0.5676	0.50	0.5270	0.8274	0.6084	0.8525
Q_3, Q_2, P_3, P_2, P_1	0.4376	0.5137	0.5454	0.7499	0.6264	0.7859
Q_3, Q_1, P_3, P_2, P_1	0.4463	0.4941	0.5332	0.7509	0.6137	0.7634
Q_2, Q_1, P_3, P_2, P_1	0.6175	0.4940	0.5561	0.8159	0.5996	0.8451
$Q_3, Q_2, Q_1, P_3, P_2, P_1$	0.5047	0.4996	0.5342	0.8102	0.6133	0.8504

Table 16: The sensitivities achieved across the combination search by each of the six classification methods.

Input combination	Classification method					
	NB	LR	SVM	RF	MLP	GB
Q_3	0.5731	0.5544	0.4823	0.5742	0.5901	0.5596
Q_2	0.4444	0.4890	0.4176	0.7615	0.6429	0.7445
Q_1	0.3032	0.5168	0.4462	0.7905	0.8099	0.7714
P_3	0.5105	0.4921	0.4920	0.5560	0.6038	0.5295
P_2	0.4563	0.4993	0.5814	0.5627	0.4633	0.5355
P_1	0.5672	0.5087	0.5135	0.5170	0.6254	0.4999
Q_3, Q_2	0.4192	0.5208	0.4962	0.7631	0.4624	0.7623
Q_3, Q_1	0.4499	0.4876	0.5059	0.7932	0.5676	0.7920
Q_3, P_3	0.4498	0.4945	0.5229	0.5867	0.5796	0.5722
Q_3, P_2	0.5414	0.5097	0.5359	0.5878	0.5213	0.5789
Q_3, P_1	0.3695	0.5152	0.5004	0.5706	0.4528	0.5565
Q_2, Q_1	0.4553	0.5012	0.4671	0.8507	0.6244	0.8585
Q_2, P_3	0.4512	0.5074	0.5175	0.7586	0.6807	0.7685
Q_2, P_2	0.5418	0.5094	0.5447	0.7603	0.5002	0.7679
Q_2, P_1	0.6622	0.4884	0.5436	0.7610	0.4879	0.7614
Q_1, P_3	0.4338	0.4961	0.5130	0.7800	0.4816	0.7653
Q_1, P_2	0.5303	0.4922	0.5428	0.7811	0.6224	0.7712
Q_1, P_1	0.4985	0.5010	0.5290	0.7889	0.5211	0.7880
P_3, P_2	0.5726	0.5062	0.5209	0.5707	0.4394	0.5581
P_3, P_1	0.5486	0.5011	0.5293	0.5467	0.5912	0.5309
P_2, P_1	0.5874	0.5069	0.5704	0.5633	0.4774	0.5649
Q_3, Q_2, Q_1	0.4242	0.5103	0.5348	0.8576	0.6101	0.8626
Q_3, Q_2, P_3	0.5442	0.4864	0.5319	0.7626	0.6180	0.7834
Q_3, Q_2, P_2	0.4241	0.4844	0.5334	0.7654	0.5662	0.7795
Q_3, Q_2, P_1	0.3655	0.4970	0.5014	0.7710	0.4641	0.7822
Q_3, Q_1, P_3	0.4862	0.4968	0.5152	0.7974	0.5408	0.7816
Q_3, Q_1, P_2	0.3600	0.5093	0.5464	0.7854	0.5539	0.7900
Q_3, Q_1, P_1	0.6213	0.5018	0.4945	0.7911	0.4948	0.8013
Q_3, P_3, P_2	0.4254	0.5061	0.5384	0.5879	0.5892	0.5813
Q_3, P_3, P_1	0.5358	0.4979	0.5295	0.5769	0.5186	0.5721
Q_3, P_2, P_1	0.4261	0.4874	0.5338	0.5892	0.6058	0.5866
Q_2, Q_1, P_3	0.5497	0.5069	0.5060	0.8522	0.5694	0.8519
Q_2, Q_1, P_2	0.5112	0.5029	0.5301	0.8494	0.6123	0.8585
Q_2, Q_1, P_1	0.4925	0.5040	0.5184	0.8519	0.5892	0.8569
Q_2, P_3, P_2	0.5315	0.5055	0.5156	0.7579	0.5643	0.7831
Q_2, P_3, P_1	0.3860	0.5075	0.5347	0.7476	0.5871	0.7710
Q_2, P_2, P_1	0.5220	0.5036	0.5285	0.7555	0.4595	0.7728
Q_1, P_3, P_2	0.5244	0.4987	0.5495	0.7755	0.5740	0.7667
Q_1, P_3, P_1	0.4414	0.5016	0.5125	0.7810	0.4611	0.7806
Q_1, P_2, P_1	0.5960	0.5021	0.5372	0.7782	0.5904	0.7804
P_3, P_2, P_1	0.5624	0.4981	0.5403	0.5647	0.5198	0.5745
Q_3, Q_2, Q_1, P_3	0.4471	0.4850	0.5120	0.8504	0.5532	0.8638
Q_3, Q_2, Q_1, P_2	0.5274	0.4996	0.5219	0.8527	0.5884	0.8660
Q_3, Q_2, Q_1, P_1	0.5160	0.5102	0.5076	0.8522	0.5872	0.8627
Q_3, Q_2, P_3, P_2	0.4522	0.5014	0.5138	0.7540	0.5326	0.7851
Q_3, Q_2, P_3, P_1	0.4492	0.4964	0.5243	0.7553	0.5639	0.7847
Q_3, Q_2, P_2, P_1	0.5909	0.5102	0.5302	0.7654	0.5839	0.7919
Q_3, Q_1, P_3, P_2	0.4603	0.4980	0.5218	0.7834	0.5805	0.7816
Q_3, Q_1, P_3, P_1	0.4671	0.5206	0.5444	0.7869	0.6011	0.7964
Q_3, Q_1, P_2, P_1	0.3623	0.4910	0.5348	0.7826	0.5723	0.7864
Q_3, P_3, P_2, P_1	0.5492	0.4823	0.5466	0.5870	0.5555	0.5932
Q_2, Q_1, P_3, P_2	0.5604	0.4929	0.5497	0.8441	0.5905	0.8545
Q_2, Q_1, P_3, P_1	0.6311	0.4995	0.5390	0.8468	0.5765	0.8575
Q_2, Q_1, P_2, P_1	0.5693	0.5133	0.5330	0.8469	0.6304	0.8664
Q_2, P_3, P_2, P_1	0.4992	0.4941	0.5316	0.7489	0.6018	0.7774
Q_1, P_3, P_2, P_1	0.4710	0.5003	0.5315	0.7757	0.6121	0.7826
Q_3, Q_2, Q_1, P_3, P_2	0.4877	0.5089	0.5329	0.8442	0.6003	0.8552
Q_3, Q_2, Q_1, P_3, P_1	0.5301	0.5002	0.5130	0.8504	0.5699	0.8668
Q_3, Q_2, Q_1, P_2, P_1	0.4670	0.5133	0.5317	0.8475	0.6064	0.8657
Q_3, Q_2, P_3, P_2, P_1	0.5697	0.5046	0.5234	0.7566	0.5836	0.7950
Q_3, Q_1, P_3, P_2, P_1	0.5467	0.5008	0.5302	0.7876	0.5581	0.7954
Q_2, Q_1, P_3, P_2, P_1	0.4502	0.5037	0.5278	0.8444	0.6443	0.8540
$Q_3, Q_2, Q_1, P_3, P_2, P_1$	0.4520	0.5023	0.5287	0.8427	0.60	0.8627

Table 17: The specificities achieved across the combination search by each of the six classification methods.

C PAD combination search results

The F_1 scores, sensitivities, and specificities achieved for PAD classification when using each of the six ML methods are shown in Table 18, 19, and 20 respectively.

Input combination	Classification method					
	NB	LR	SVM	RF	MLP	GB
Q_3	0.5017	0.5115	0.6645	0.8224	0.6897	0.8169
Q_2	0.5621	0.5222	0.5266	0.7127	0.4734	0.7076
Q_1	0.3927	0.4822	0.5310	0.8240	0.4713	0.8183
P_3	0.5162	0.5053	0.5182	0.5613	0.4131	0.5406
P_2	0.5030	0.4954	0.5242	0.5753	0.4741	0.5529
P_1	0.4290	0.5031	0.5038	0.5517	0.5487	0.5335
Q_3, Q_2	0.4740	0.5099	0.5926	0.8480	0.7040	0.8557
Q_3, Q_1	0.5355	0.4965	0.5786	0.8959	0.7254	0.9041
Q_3, P_3	0.4800	0.4932	0.5808	0.8050	0.6676	0.8151
Q_3, P_2	0.5118	0.4998	0.5824	0.8152	0.7057	0.8201
Q_3, P_1	0.5672	0.4979	0.5768	0.8103	0.7206	0.8221
Q_2, Q_1	0.5236	0.4962	0.5239	0.8556	0.5610	0.8637
Q_2, P_3	0.4929	0.4980	0.5069	0.7134	0.6117	0.7200
Q_2, P_2	0.5323	0.4956	0.5133	0.7126	0.5233	0.7255
Q_2, P_1	0.4602	0.5075	0.5222	0.7117	0.5585	0.7221
Q_1, P_3	0.5293	0.5116	0.5420	0.8136	0.5602	0.8204
Q_1, P_2	0.5335	0.4926	0.5406	0.8187	0.5818	0.8314
Q_1, P_1	0.5549	0.5011	0.5417	0.8181	0.6514	0.8307
P_3, P_2	0.4829	0.4996	0.5319	0.5810	0.5386	0.5733
P_3, P_1	0.4823	0.4976	0.5142	0.5624	0.5141	0.5559
P_2, P_1	0.5434	0.5035	0.5145	0.5904	0.4662	0.6002
Q_3, Q_2, Q_1	0.5209	0.4891	0.5619	0.9061	0.7004	0.9168
Q_3, Q_2, P_3	0.4717	0.5146	0.5605	0.8370	0.6864	0.8556
Q_3, Q_2, P_2	0.4651	0.5049	0.5640	0.8424	0.7074	0.8606
Q_3, Q_2, P_1	0.4643	0.5064	0.5610	0.8408	0.7040	0.8592
Q_3, Q_1, P_3	0.4947	0.4976	0.5679	0.8833	0.7148	0.9009
Q_3, Q_1, P_2	0.5615	0.4984	0.5741	0.8858	0.7100	0.9022
Q_3, Q_1, P_1	0.4149	0.4941	0.5760	0.8850	0.7361	0.9046
Q_3, P_3, P_2	0.4800	0.5065	0.5598	0.8005	0.6804	0.8215
Q_3, P_3, P_1	0.5214	0.5050	0.5642	0.8005	0.6886	0.8179
Q_3, P_2, P_1	0.4792	0.5065	0.5630	0.8004	0.7104	0.8178
Q_2, Q_1, P_3	0.5208	0.5006	0.5334	0.8469	0.6300	0.8617
Q_2, Q_1, P_2	0.4874	0.4974	0.5318	0.8472	0.5992	0.8703
Q_2, Q_1, P_1	0.5340	0.4938	0.5311	0.8472	0.6472	0.8682
Q_2, P_3, P_2	0.5306	0.4996	0.5162	0.7147	0.5581	0.7379
Q_2, P_3, P_1	0.5012	0.4989	0.5152	0.7062	0.5165	0.7311
Q_2, P_2, P_1	0.5165	0.4983	0.5232	0.7118	0.5659	0.7322
Q_1, P_3, P_2	0.5324	0.4941	0.5382	0.8086	0.6117	0.8302
Q_1, P_3, P_1	0.4632	0.5047	0.5322	0.8116	0.6127	0.8324
Q_1, P_2, P_1	0.4524	0.4930	0.5429	0.8146	0.6441	0.8380
P_3, P_2, P_1	0.5016	0.5023	0.5262	0.5838	0.5654	0.6078
Q_3, Q_2, Q_1, P_3	0.5480	0.5086	0.5600	0.8992	0.6988	0.9138
Q_3, Q_2, Q_1, P_2	0.4505	0.4997	0.5564	0.8997	0.7017	0.9164
Q_3, Q_2, Q_1, P_1	0.4973	0.5053	0.5601	0.8990	0.7030	0.9196
Q_3, Q_2, P_3, P_2	0.3998	0.4993	0.5601	0.8376	0.6688	0.8612
Q_3, Q_2, P_3, P_1	0.5253	0.4973	0.5558	0.8330	0.6738	0.8556
Q_3, Q_2, P_2, P_1	0.4726	0.4972	0.5650	0.8385	0.6811	0.8597
Q_3, Q_1, P_3, P_2	0.5030	0.4976	0.5684	0.8803	0.6845	0.8999
Q_3, Q_1, P_3, P_1	0.5189	0.5019	0.5595	0.8839	0.6849	0.9013
Q_3, Q_1, P_2, P_1	0.5692	0.4994	0.5715	0.8805	0.6962	0.9025
Q_3, P_3, P_2, P_1	0.4801	0.4991	0.5576	0.7940	0.6746	0.8170
Q_2, Q_1, P_3, P_2	0.4681	0.4966	0.5404	0.8417	0.6239	0.8624
Q_2, Q_1, P_3, P_1	0.5009	0.5015	0.5278	0.8378	0.6146	0.8677
Q_2, Q_1, P_2, P_1	0.5278	0.4979	0.5304	0.8433	0.6327	0.8690
Q_2, P_3, P_2, P_1	0.5242	0.5024	0.5180	0.7022	0.5806	0.7376
Q_1, P_3, P_2, P_1	0.4996	0.5033	0.5355	0.8087	0.6158	0.8328
Q_3, Q_2, Q_1, P_3, P_2	0.5012	0.5006	0.5495	0.8971	0.6889	0.9169
Q_3, Q_2, Q_1, P_3, P_1	0.5025	0.4969	0.5562	0.8952	0.6887	0.9151
Q_3, Q_2, Q_1, P_2, P_1	0.5023	0.5019	0.5502	0.8969	0.6895	0.9170
Q_3, Q_2, P_3, P_2, P_1	0.4946	0.4923	0.5488	0.8279	0.6545	0.8597
Q_3, Q_1, P_3, P_2, P_1	0.4489	0.4972	0.5666	0.8758	0.6688	0.9042
Q_2, Q_1, P_3, P_2, P_1	0.5377	0.4995	0.5391	0.8389	0.6154	0.8655
$Q_3, Q_2, Q_1, P_3, P_2, P_1$	0.4479	0.4974	0.5573	0.8935	0.6681	0.9187

Table 18: The F_1 scores achieved across the combination search by each of the six classification methods.

Input combination	Classification method					
	NB	LR	SVM	RF	MLP	GB
Q_3	0.3598	0.5048	0.6806	0.8219	0.5998	0.8188
Q_2	0.5441	0.4878	0.5879	0.6858	0.5536	0.6922
Q_1	0.5735	0.5026	0.6065	0.8126	0.5959	0.8140
P_3	0.4246	0.4935	0.5472	0.5358	0.6388	0.5425
P_2	0.4565	0.4985	0.5368	0.5532	0.5572	0.5576
P_1	0.6253	0.5001	0.5571	0.5245	0.3899	0.5261
Q_3, Q_2	0.5595	0.4912	0.6297	0.8414	0.7176	0.8532
Q_3, Q_1	0.4753	0.5087	0.6324	0.8825	0.7460	0.8950
Q_3, P_3	0.6086	0.5025	0.5980	0.8021	0.6523	0.8173
Q_3, P_2	0.3310	0.4895	0.5919	0.8089	0.7679	0.8269
Q_3, P_1	0.3079	0.5280	0.6021	0.8051	0.7461	0.8266
Q_2, Q_1	0.4323	0.4902	0.5878	0.8346	0.6016	0.8521
Q_2, P_3	0.5419	0.4877	0.5744	0.6826	0.2813	0.7126
Q_2, P_2	0.5505	0.5051	0.5776	0.6862	0.5169	0.7275
Q_2, P_1	0.6100	0.4976	0.5697	0.6875	0.4716	0.7127
Q_1, P_3	0.3309	0.4971	0.5476	0.8001	0.5911	0.8168
Q_1, P_2	0.5495	0.5063	0.5827	0.8019	0.5508	0.8288
Q_1, P_1	0.3834	0.4930	0.5778	0.8059	0.6787	0.8272
P_3, P_2	0.4789	0.4946	0.5458	0.5569	0.5443	0.5709
P_3, P_1	0.5309	0.5066	0.5642	0.5425	0.5406	0.5484
P_2, P_1	0.5325	0.4961	0.5863	0.5651	0.6096	0.5998
Q_3, Q_2, Q_1	0.4948	0.5163	0.5976	0.8885	0.7801	0.9055
Q_3, Q_2, P_3	0.3895	0.4985	0.5568	0.8323	0.7286	0.8572
Q_3, Q_2, P_2	0.5612	0.5051	0.5851	0.8388	0.6953	0.8545
Q_3, Q_2, P_1	0.4521	0.4890	0.5787	0.8278	0.7259	0.8559
Q_3, Q_1, P_3	0.5637	0.5045	0.5826	0.8707	0.7050	0.8913
Q_3, Q_1, P_2	0.4240	0.5030	0.5974	0.8710	0.7409	0.8923
Q_3, Q_1, P_1	0.6578	0.5094	0.6104	0.8663	0.6902	0.8928
Q_3, P_3, P_2	0.3869	0.4995	0.5834	0.7984	0.6967	0.8211
Q_3, P_3, P_1	0.2820	0.5009	0.5706	0.7914	0.6994	0.8208
Q_3, P_2, P_1	0.5814	0.4880	0.5824	0.7970	0.6789	0.8163
Q_2, Q_1, P_3	0.3260	0.4775	0.5663	0.8303	0.5969	0.8540
Q_2, Q_1, P_2	0.4239	0.4959	0.5625	0.8309	0.6028	0.8636
Q_2, Q_1, P_1	0.3205	0.5176	0.5610	0.8289	0.6418	0.8595
Q_2, P_3, P_2	0.4276	0.4900	0.5714	0.6920	0.5968	0.7328
Q_2, P_3, P_1	0.5554	0.4896	0.5560	0.6859	0.6252	0.7136
Q_2, P_2, P_1	0.4250	0.5134	0.5664	0.6845	0.5546	0.7245
Q_1, P_3, P_2	0.5668	0.4987	0.5330	0.7935	0.5752	0.8208
Q_1, P_3, P_1	0.4876	0.5104	0.5537	0.7998	0.6082	0.8287
Q_1, P_2, P_1	0.6109	0.4885	0.5572	0.8022	0.5978	0.8313
P_3, P_2, P_1	0.3959	0.4901	0.5652	0.5688	0.5532	0.6022
Q_3, Q_2, Q_1, P_3	0.3678	0.4879	0.5510	0.8819	0.7136	0.9035
Q_3, Q_2, Q_1, P_2	0.4522	0.5111	0.5909	0.8868	0.7224	0.9085
Q_3, Q_2, Q_1, P_1	0.5593	0.4867	0.5680	0.8846	0.7250	0.9068
Q_3, Q_2, P_3, P_2	0.5688	0.4972	0.5879	0.8231	0.7166	0.8574
Q_3, Q_2, P_3, P_1	0.4517	0.5112	0.5707	0.8201	0.7036	0.8504
Q_3, Q_2, P_2, P_1	0.5414	0.4904	0.5642	0.8247	0.7091	0.8526
Q_3, Q_1, P_3, P_2	0.6603	0.4851	0.5512	0.8655	0.7055	0.8936
Q_3, Q_1, P_3, P_1	0.3708	0.4993	0.5781	0.8655	0.7178	0.8951
Q_3, Q_1, P_2, P_1	0.4094	0.4967	0.5752	0.8612	0.7042	0.8926
Q_3, P_3, P_2, P_1	0.5180	0.5097	0.5724	0.7834	0.6593	0.8182
Q_2, Q_1, P_3, P_2	0.3984	0.4901	0.5564	0.8199	0.6451	0.8568
Q_2, Q_1, P_3, P_1	0.3787	0.5159	0.5556	0.8243	0.6639	0.8587
Q_2, Q_1, P_2, P_1	0.4432	0.5153	0.5587	0.8324	0.6442	0.8633
Q_2, P_3, P_2, P_1	0.4612	0.4878	0.5385	0.6811	0.5837	0.7262
Q_1, P_3, P_2, P_1	0.4762	0.4917	0.5679	0.7953	0.6449	0.8315
Q_3, Q_2, Q_1, P_3, P_2	0.3675	0.5049	0.5659	0.8802	0.6844	0.9133
Q_3, Q_2, Q_1, P_3, P_1	0.3552	0.4925	0.5784	0.8766	0.6848	0.9073
Q_3, Q_2, Q_1, P_2, P_1	0.4635	0.4996	0.5754	0.8829	0.6910	0.9041
Q_3, Q_2, P_3, P_2, P_1	0.4797	0.5169	0.5518	0.8142	0.6891	0.8544
Q_3, Q_1, P_3, P_2, P_1	0.5274	0.5069	0.5507	0.8625	0.6738	0.8986
Q_2, Q_1, P_3, P_2, P_1	0.3947	0.4911	0.5493	0.8258	0.6190	0.8556
$Q_3, Q_2, Q_1, P_3, P_2, P_1$	0.6385	0.4859	0.5511	0.8813	0.6588	0.9102

Table 19: The sensitivities achieved across the combination search by each of the six classification methods.

Input combination	Classification method					
	NB	LR	SVM	RF	MLP	GB
Q_3	0.5493	0.5139	0.6566	0.8228	0.7371	0.8157
Q_2	0.5692	0.5344	0.5047	0.7276	0.4486	0.7161
Q_1	0.3486	0.4758	0.5038	0.8320	0.4329	0.8214
P_3	0.5481	0.5093	0.5081	0.5713	0.3544	0.5399
P_2	0.5187	0.4945	0.5198	0.5843	0.4484	0.5512
P_1	0.3754	0.5042	0.4859	0.5622	0.6088	0.5362
Q_3, Q_2	0.4475	0.5164	0.5770	0.8529	0.6967	0.8576
Q_3, Q_1	0.5576	0.4926	0.5568	0.9068	0.7137	0.9117
Q_3, P_3	0.4395	0.4902	0.5738	0.8070	0.6754	0.8137
Q_3, P_2	0.5740	0.5033	0.5785	0.8196	0.6718	0.8155
Q_3, P_1	0.6699	0.4880	0.5666	0.8140	0.7063	0.8190
Q_2, Q_1	0.5561	0.4983	0.5013	0.8714	0.5452	0.8726
Q_2, P_3	0.4769	0.5015	0.4840	0.7305	0.7573	0.7243
Q_2, P_2	0.5257	0.4926	0.4912	0.7273	0.5257	0.7245
Q_2, P_1	0.4155	0.5109	0.5055	0.7252	0.5922	0.7275
Q_1, P_3	0.6008	0.5166	0.5400	0.8229	0.5482	0.8230
Q_1, P_2	0.5277	0.4882	0.5251	0.8305	0.5946	0.8334
Q_1, P_1	0.6209	0.5039	0.5284	0.8266	0.6383	0.8333
P_3, P_2	0.4842	0.5013	0.5269	0.5910	0.5365	0.5743
P_3, P_1	0.4669	0.4947	0.4970	0.5703	0.5050	0.5589
P_2, P_1	0.5476	0.5061	0.4897	0.6010	0.4227	0.6004
Q_3, Q_2, Q_1	0.5302	0.4803	0.5480	0.9208	0.6575	0.9265
Q_3, Q_2, P_3	0.4972	0.5203	0.5620	0.8405	0.6644	0.8545
Q_3, Q_2, P_2	0.4360	0.5049	0.5558	0.8451	0.7141	0.8653
Q_3, Q_2, P_1	0.4681	0.5123	0.5541	0.8504	0.6922	0.8618
Q_3, Q_1, P_3	0.4721	0.4954	0.5622	0.8933	0.7204	0.9088
Q_3, Q_1, P_2	0.6153	0.4970	0.5648	0.8976	0.6931	0.9104
Q_3, Q_1, P_1	0.3514	0.4892	0.5621	0.9000	0.7629	0.9144
Q_3, P_3, P_2	0.5095	0.5090	0.5507	0.8020	0.6720	0.8218
Q_3, P_3, P_1	0.6059	0.5064	0.5617	0.8066	0.6830	0.8159
Q_3, P_2, P_1	0.4470	0.5129	0.5555	0.8028	0.7279	0.8189
Q_2, Q_1, P_3	0.5894	0.5084	0.5215	0.8592	0.6453	0.8677
Q_2, Q_1, P_2	0.5079	0.4979	0.5207	0.8593	0.5977	0.8755
Q_2, Q_1, P_1	0.6118	0.4860	0.5203	0.8607	0.6498	0.8749
Q_2, P_3, P_2	0.5679	0.5029	0.4971	0.7274	0.5432	0.7410
Q_2, P_3, P_1	0.4831	0.5021	0.5011	0.7173	0.4787	0.7413
Q_2, P_2, P_1	0.5484	0.4934	0.5080	0.7270	0.5704	0.7368
Q_1, P_3, P_2	0.5200	0.4927	0.5402	0.8190	0.6278	0.8369
Q_1, P_3, P_1	0.4559	0.5028	0.5245	0.8198	0.6148	0.8351
Q_1, P_2, P_1	0.4061	0.4945	0.5376	0.8232	0.6662	0.8430
P_3, P_2, P_1	0.5371	0.5064	0.5123	0.5900	0.5703	0.6103
Q_3, Q_2, Q_1, P_3	0.6161	0.5157	0.5636	0.9135	0.6910	0.9226
Q_3, Q_2, Q_1, P_2	0.4501	0.4960	0.5432	0.9104	0.6906	0.9231
Q_3, Q_2, Q_1, P_1	0.4769	0.5116	0.5571	0.9108	0.6911	0.9306
Q_3, Q_2, P_3, P_2	0.3576	0.5001	0.5493	0.8481	0.6448	0.8642
Q_3, Q_2, P_3, P_1	0.5516	0.4927	0.5502	0.8423	0.6587	0.8596
Q_3, Q_2, P_2, P_1	0.4514	0.4995	0.5654	0.8485	0.6667	0.8652
Q_3, Q_1, P_3, P_2	0.4502	0.5018	0.5753	0.8920	0.6736	0.9052
Q_3, Q_1, P_3, P_1	0.5708	0.5029	0.5523	0.8986	0.6678	0.9065
Q_3, Q_1, P_2, P_1	0.6328	0.5003	0.5701	0.8957	0.6920	0.9107
Q_3, P_3, P_2, P_1	0.4682	0.4956	0.5519	0.8011	0.6825	0.8163
Q_2, Q_1, P_3, P_2	0.4894	0.4988	0.5346	0.8577	0.6144	0.8667
Q_2, Q_1, P_3, P_1	0.5418	0.4968	0.5179	0.8477	0.5928	0.8747
Q_2, Q_1, P_2, P_1	0.5582	0.4922	0.5202	0.8513	0.6274	0.8734
Q_2, P_3, P_2, P_1	0.5467	0.5073	0.5109	0.7137	0.5794	0.7443
Q_1, P_3, P_2, P_1	0.5075	0.5073	0.5237	0.8179	0.6029	0.8338
Q_3, Q_2, Q_1, P_3, P_2	0.5460	0.4992	0.5434	0.9110	0.6913	0.9201
Q_3, Q_2, Q_1, P_3, P_1	0.5520	0.4984	0.5477	0.9103	0.6909	0.9218
Q_3, Q_2, Q_1, P_2, P_1	0.5154	0.5028	0.5407	0.9084	0.6888	0.9281
Q_3, Q_2, P_3, P_2, P_1	0.4996	0.4843	0.5478	0.8377	0.6378	0.8638
Q_3, Q_1, P_3, P_2, P_1	0.4262	0.4940	0.5729	0.8862	0.6664	0.9089
Q_2, Q_1, P_3, P_2, P_1	0.5904	0.5024	0.5354	0.8485	0.6138	0.8732
$Q_3, Q_2, Q_1, P_3, P_2, P_1$	0.3930	0.5013	0.5597	0.9035	0.6729	0.9261

Table 20: The specificities achieved across the combination search by each of the six classification methods.

D AAA combination search results

The F_1 scores, sensitivities, and specificities achieved for AAA classification when using each of the six ML methods are shown in Table 21, 22, and 23 respectively.

Input combination	Classification method					
	NB	LR	SVM	RF	MLP	GB
Q_3	0.4670	0.4881	0.8454	0.9095	0.8606	0.9294
Q_2	0.5754	0.4952	0.8246	0.9516	0.9092	0.9640
Q_1	0.4440	0.4843	0.9481	0.9741	0.9697	0.9805
P_3	0.4999	0.5102	0.8664	0.9027	0.8692	0.9226
P_2	0.5782	0.4944	0.8717	0.9087	0.8793	0.9311
P_1	0.4790	0.4826	0.8212	0.8771	0.8416	0.8884
Q_3, Q_2	0.3850	0.4983	0.8895	0.9753	0.9249	0.9843
Q_3, Q_1	0.4982	0.5029	0.9521	0.9840	0.9749	0.9919
Q_3, P_3	0.5126	0.4960	0.9215	0.9483	0.9249	0.9767
Q_3, P_2	0.6111	0.4958	0.9355	0.9543	0.9385	0.9770
Q_3, P_1	0.4737	0.4971	0.9286	0.9498	0.9448	0.9702
Q_2, Q_1	0.5523	0.4970	0.9523	0.9868	0.9718	0.9928
Q_2, P_3	0.5080	0.4994	0.9305	0.9604	0.9430	0.9805
Q_2, P_2	0.4756	0.4996	0.9371	0.9712	0.9552	0.9849
Q_2, P_1	0.4032	0.4975	0.9168	0.9689	0.9413	0.9828
Q_1, P_3	0.5350	0.5046	0.9630	0.9808	0.9741	0.9870
Q_1, P_2	0.4613	0.4981	0.9681	0.9820	0.9756	0.9900
Q_1, P_1	0.4909	0.5003	0.9747	0.9798	0.9801	0.9852
P_3, P_2	0.5343	0.5018	0.9247	0.9335	0.9305	0.9677
P_3, P_1	0.4857	0.5078	0.9321	0.9345	0.9311	0.9675
P_2, P_1	0.5431	0.5039	0.9213	0.9365	0.9405	0.9625
Q_3, Q_2, Q_1	0.4890	0.5164	0.9603	0.9912	0.9729	0.9962
Q_3, Q_2, P_3	0.5485	0.4993	0.9452	0.9771	0.9436	0.9905
Q_3, Q_2, P_2	0.5359	0.4998	0.9542	0.9791	0.9568	0.9910
Q_3, Q_2, P_1	0.4374	0.5070	0.9518	0.9803	0.9503	0.9906
Q_3, Q_1, P_3	0.5193	0.5085	0.9663	0.9861	0.9740	0.9936
Q_3, Q_1, P_2	0.5325	0.5034	0.9747	0.9884	0.9784	0.9939
Q_3, Q_1, P_1	0.4819	0.4943	0.9781	0.9850	0.9796	0.9936
Q_3, P_3, P_2	0.4106	0.4991	0.9479	0.9586	0.9434	0.9807
Q_3, P_3, P_1	0.4291	0.4901	0.9560	0.9598	0.9491	0.9846
Q_3, P_2, P_1	0.4537	0.4948	0.9492	0.9647	0.9515	0.9804
Q_2, Q_1, P_3	0.5071	0.5051	0.9685	0.9877	0.9795	0.9944
Q_2, Q_1, P_2	0.4853	0.4951	0.9724	0.9893	0.9797	0.9957
Q_2, Q_1, P_1	0.4459	0.4994	0.9752	0.9885	0.9816	0.9952
Q_2, P_3, P_2	0.4060	0.4932	0.9566	0.9714	0.9576	0.9873
Q_2, P_3, P_1	0.5857	0.4972	0.9577	0.9722	0.9582	0.9882
Q_2, P_2, P_1	0.4776	0.5030	0.9497	0.9755	0.9671	0.9892
Q_1, P_3, P_2	0.4224	0.4974	0.9729	0.9823	0.9788	0.9904
Q_1, P_3, P_1	0.4944	0.4987	0.9747	0.9813	0.9797	0.9897
Q_1, P_2, P_1	0.5362	0.5051	0.9756	0.9828	0.9827	0.9917
P_3, P_2, P_1	0.4406	0.5001	0.9479	0.9455	0.9517	0.9750
Q_3, Q_2, Q_1, P_3	0.5284	0.5135	0.9711	0.9914	0.9756	0.9965
Q_3, Q_2, Q_1, P_2	0.5279	0.5066	0.9784	0.9923	0.9794	0.9972
Q_3, Q_2, Q_1, P_1	0.4331	0.4983	0.9790	0.9903	0.9792	0.9961
Q_3, Q_2, P_3, P_2	0.5090	0.5041	0.9636	0.9797	0.9582	0.9930
Q_3, Q_2, P_3, P_1	0.5250	0.4963	0.9665	0.9784	0.9633	0.9922
Q_3, Q_2, P_2, P_1	0.4600	0.4887	0.9646	0.9829	0.9724	0.9937
Q_3, Q_1, P_3, P_2	0.4994	0.5003	0.9759	0.9880	0.9771	0.9939
Q_3, Q_1, P_3, P_1	0.5058	0.5060	0.9779	0.9867	0.9782	0.9942
Q_3, Q_1, P_2, P_1	0.4981	0.4974	0.9781	0.9869	0.9778	0.9950
Q_3, P_3, P_2, P_1	0.4679	0.5050	0.9634	0.9651	0.9595	0.9856
Q_2, Q_1, P_3, P_2	0.4910	0.4989	0.9776	0.9901	0.9759	0.9954
Q_2, Q_1, P_3, P_1	0.4893	0.5041	0.9794	0.9892	0.9772	0.9948
Q_2, Q_1, P_2, P_1	0.4849	0.4994	0.9771	0.9911	0.9800	0.9957
Q_2, P_3, P_2, P_1	0.4963	0.5081	0.9644	0.9748	0.9684	0.9903
Q_1, P_3, P_2, P_1	0.5090	0.5054	0.9763	0.9857	0.9788	0.9910
Q_3, Q_2, Q_1, P_3, P_2	0.4588	0.4997	0.9781	0.9915	0.9739	0.9970
Q_3, Q_2, Q_1, P_3, P_1	0.5224	0.4957	0.9800	0.9920	0.9767	0.9970
Q_3, Q_2, Q_1, P_2, P_1	0.5003	0.4947	0.9823	0.9912	0.9808	0.9966
Q_3, Q_2, P_3, P_2, P_1	0.4667	0.4900	0.9708	0.9828	0.9668	0.9948
Q_3, Q_1, P_3, P_2, P_1	0.5322	0.4962	0.9801	0.9874	0.9775	0.9938
Q_2, Q_1, P_3, P_2, P_1	0.4450	0.5064	0.9801	0.9892	0.9808	0.9961
$Q_3, Q_2, Q_1, P_3, P_2, P_1$	0.5083	0.4991	0.9820	0.9912	0.9785	0.9970

Table 21: The F_1 scores achieved across the combination search by each of the six classification methods.

Input combination	Classification method					
	NB	LR	SVM	RF	MLP	GB
Q_3	0.5683	0.5120	0.8568	0.8878	0.8661	0.9300
Q_2	0.5738	0.5089	0.8136	0.9355	0.9100	0.9638
Q_1	0.4451	0.4962	0.9517	0.9654	0.9673	0.9799
P_3	0.4846	0.5035	0.8785	0.8765	0.8660	0.9202
P_2	0.4451	0.5110	0.8712	0.9005	0.8818	0.9352
P_1	0.6616	0.4902	0.8491	0.8514	0.8308	0.8770
Q_3, Q_2	0.5927	0.4676	0.8868	0.9652	0.9308	0.9835
Q_3, Q_1	0.5541	0.5333	0.9508	0.9757	0.9747	0.9907
Q_3, P_3	0.4269	0.4894	0.9222	0.9282	0.9266	0.9746
Q_3, P_2	0.4746	0.5016	0.9325	0.9382	0.9379	0.9819
Q_3, P_1	0.5850	0.4760	0.9213	0.9317	0.9462	0.9694
Q_2, Q_1	0.2504	0.5034	0.9534	0.9810	0.9738	0.9919
Q_2, P_3	0.4111	0.4591	0.9285	0.9464	0.9439	0.9793
Q_2, P_2	0.5865	0.5093	0.9345	0.9604	0.9544	0.9836
Q_2, P_1	0.5669	0.4940	0.9227	0.9552	0.9471	0.9817
Q_1, P_3	0.4266	0.4741	0.9626	0.9729	0.9743	0.9850
Q_1, P_2	0.5075	0.4991	0.9664	0.9743	0.9780	0.9895
Q_1, P_1	0.5143	0.5055	0.9742	0.9715	0.9806	0.9841
P_3, P_2	0.4414	0.4981	0.9287	0.9209	0.9379	0.9673
P_3, P_1	0.5355	0.4956	0.9461	0.9109	0.9337	0.9631
P_2, P_1	0.4090	0.4957	0.9311	0.9260	0.9359	0.9596
Q_3, Q_2, Q_1	0.6548	0.5014	0.9592	0.9864	0.9760	0.9954
Q_3, Q_2, P_3	0.4363	0.4885	0.9445	0.9689	0.9482	0.9897
Q_3, Q_2, P_2	0.5720	0.5284	0.9506	0.9704	0.9620	0.9904
Q_3, Q_2, P_1	0.4962	0.5110	0.9455	0.9723	0.9511	0.9914
Q_3, Q_1, P_3	0.5329	0.4857	0.9666	0.9793	0.9774	0.9913
Q_3, Q_1, P_2	0.3570	0.4931	0.9701	0.9820	0.9794	0.9929
Q_3, Q_1, P_1	0.3667	0.5022	0.9771	0.9755	0.9805	0.9924
Q_3, P_3, P_2	0.6250	0.5064	0.9434	0.9445	0.9426	0.9822
Q_3, P_3, P_1	0.4716	0.4865	0.9564	0.9413	0.9473	0.9843
Q_3, P_2, P_1	0.5103	0.4982	0.9447	0.9522	0.9575	0.9819
Q_2, Q_1, P_3	0.4499	0.4986	0.9676	0.9815	0.9797	0.9933
Q_2, Q_1, P_2	0.6389	0.4936	0.9689	0.9838	0.9795	0.9947
Q_2, Q_1, P_1	0.6675	0.5043	0.9741	0.9817	0.9811	0.9945
Q_2, P_3, P_2	0.5890	0.4948	0.9564	0.9609	0.9598	0.9864
Q_2, P_3, P_1	0.4238	0.5033	0.9606	0.9619	0.9578	0.9868
Q_2, P_2, P_1	0.5582	0.5024	0.9540	0.9660	0.9686	0.9881
Q_1, P_3, P_2	0.5561	0.4904	0.9703	0.9736	0.9786	0.9898
Q_1, P_3, P_1	0.6229	0.5165	0.9753	0.9725	0.9799	0.9881
Q_1, P_2, P_1	0.4489	0.5084	0.9753	0.9750	0.9837	0.9896
P_3, P_2, P_1	0.6036	0.5139	0.9563	0.9278	0.9522	0.9726
Q_3, Q_2, Q_1, P_3	0.4318	0.5058	0.9684	0.9870	0.9803	0.9953
Q_3, Q_2, Q_1, P_2	0.5271	0.4841	0.9751	0.9879	0.9791	0.9959
Q_3, Q_2, Q_1, P_1	0.6257	0.4871	0.9768	0.9848	0.9794	0.9944
Q_3, Q_2, P_3, P_2	0.4330	0.5113	0.9615	0.9692	0.9620	0.9922
Q_3, Q_2, P_3, P_1	0.4955	0.4973	0.9639	0.9675	0.9661	0.9925
Q_3, Q_2, P_2, P_1	0.4783	0.4925	0.9610	0.9737	0.9660	0.9930
Q_3, Q_1, P_3, P_2	0.4914	0.4957	0.9741	0.9818	0.9795	0.9932
Q_3, Q_1, P_3, P_1	0.5768	0.5028	0.9778	0.9794	0.9788	0.9928
Q_3, Q_1, P_2, P_1	0.4613	0.4924	0.9749	0.9805	0.9771	0.9940
Q_3, P_3, P_2, P_1	0.6938	0.5114	0.9619	0.9516	0.9633	0.9856
Q_2, Q_1, P_3, P_2	0.5969	0.4915	0.9770	0.9861	0.9772	0.9944
Q_2, Q_1, P_3, P_1	0.5361	0.5044	0.9800	0.9846	0.9770	0.9938
Q_2, Q_1, P_2, P_1	0.5999	0.5042	0.9753	0.9867	0.9815	0.9944
Q_2, P_3, P_2, P_1	0.4892	0.4885	0.9676	0.9650	0.9693	0.9887
Q_1, P_3, P_2, P_1	0.3810	0.5027	0.9761	0.9790	0.9791	0.9887
Q_3, Q_2, Q_1, P_3, P_2	0.5180	0.5006	0.9749	0.9866	0.9752	0.9959
Q_3, Q_2, Q_1, P_3, P_1	0.4600	0.4811	0.9805	0.9873	0.9794	0.9963
Q_3, Q_2, Q_1, P_2, P_1	0.4965	0.5034	0.9824	0.9870	0.9808	0.9952
Q_3, Q_2, P_3, P_2, P_1	0.4020	0.5030	0.9704	0.9745	0.9692	0.9944
Q_3, Q_1, P_3, P_2, P_1	0.4284	0.5086	0.9809	0.9804	0.9763	0.9925
Q_2, Q_1, P_3, P_2, P_1	0.5795	0.4863	0.9812	0.9836	0.9811	0.9949
$Q_3, Q_2, Q_1, P_3, P_2, P_1$	0.4242	0.5024	0.9802	0.9861	0.9778	0.9959

Table 22: The sensitivities achieved across the combination search by each of the six classification methods.

Input combination	Classification method					
	NB	LR	SVM	RF	MLP	GB
Q_3	0.4362	0.4805	0.8371	0.9276	0.8565	0.9290
Q_2	0.5761	0.4908	0.8324	0.9663	0.9087	0.9643
Q_1	0.4437	0.4806	0.9450	0.9825	0.9720	0.9811
P_3	0.5050	0.5126	0.8572	0.9244	0.8718	0.9248
P_2	0.6324	0.4890	0.8722	0.9156	0.8775	0.9277
P_1	0.4215	0.4803	0.8018	0.8972	0.8496	0.8976
Q_3, Q_2	0.3355	0.5086	0.8917	0.9851	0.9200	0.9851
Q_3, Q_1	0.4797	0.4927	0.9533	0.9922	0.9751	0.9931
Q_3, P_3	0.5422	0.4982	0.9210	0.9666	0.9235	0.9788
Q_3, P_2	0.6712	0.4939	0.9383	0.9691	0.9392	0.9724
Q_3, P_1	0.4392	0.5041	0.9351	0.9662	0.9436	0.97103
Q_2, Q_1	0.6675	0.4949	0.9514	0.9926	0.9701	0.9938
Q_2, P_3	0.5410	0.5129	0.9324	0.9735	0.9423	0.9817
Q_2, P_2	0.4411	0.4964	0.9394	0.9815	0.9561	0.9862
Q_2, P_1	0.3619	0.4987	0.9119	0.9819	0.9363	0.9840
Q_1, P_3	0.5747	0.5149	0.9635	0.9885	0.9741	0.9890
Q_1, P_2	0.4475	0.4979	0.9697	0.9896	0.9734	0.9906
Q_1, P_1	0.4834	0.4986	0.9753	0.9879	0.9797	0.9863
P_3, P_2	0.5682	0.5031	0.9213	0.9447	0.9241	0.9681
P_3, P_1	0.4698	0.5120	0.9199	0.9552	0.9289	0.9718
P_2, P_1	0.5932	0.5067	0.9130	0.9459	0.9446	0.9652
Q_3, Q_2, Q_1	0.4354	0.5217	0.9615	0.9961	0.9700	0.9970
Q_3, Q_2, P_3	0.5910	0.5030	0.9460	0.9850	0.9396	0.9914
Q_3, Q_2, P_2	0.5227	0.4904	0.9575	0.9876	0.9522	0.9917
Q_3, Q_2, P_1	0.4210	0.5057	0.9576	0.9880	0.9496	0.9899
Q_3, Q_1, P_3	0.5146	0.5163	0.9662	0.9928	0.9708	0.9960
Q_3, Q_1, P_2	0.5963	0.5069	0.9792	0.9947	0.9775	0.9950
Q_3, Q_1, P_1	0.5186	0.4918	0.9792	0.9944	0.9789	0.9949
Q_3, P_3, P_2	0.3553	0.4967	0.9520	0.9716	0.9442	0.9794
Q_3, P_3, P_1	0.4176	0.4913	0.9557	0.9769	0.9509	0.9850
Q_3, P_2, P_1	0.4371	0.4938	0.9533	0.9764	0.9461	0.9791
Q_2, Q_1, P_3	0.5266	0.5074	0.9695	0.9939	0.9794	0.9956
Q_2, Q_1, P_2	0.4362	0.4957	0.9758	0.9948	0.9799	0.9967
Q_2, Q_1, P_1	0.3824	0.4979	0.9764	0.9952	0.9822	0.9959
Q_2, P_3, P_2	0.3595	0.4928	0.9568	0.9814	0.9557	0.9882
Q_2, P_3, P_1	0.6529	0.4952	0.9552	0.9821	0.9586	0.9896
Q_2, P_2, P_1	0.4524	0.5033	0.9460	0.9847	0.9658	0.9903
Q_1, P_3, P_2	0.3867	0.4998	0.9754	0.9908	0.9791	0.9910
Q_1, P_3, P_1	0.4523	0.4929	0.9743	0.9898	0.9796	0.9913
Q_1, P_2, P_1	0.5683	0.5040	0.9759	0.9904	0.9819	0.9939
P_3, P_2, P_1	0.3946	0.4955	0.9405	0.9614	0.9513	0.9774
Q_3, Q_2, Q_1, P_3	0.5631	0.5162	0.9738	0.9958	0.9713	0.9977
Q_3, Q_2, Q_1, P_2	0.5282	0.5143	0.9816	0.9967	0.9797	0.9986
Q_3, Q_2, Q_1, P_1	0.3799	0.5021	0.9813	0.9958	0.9792	0.9978
Q_3, Q_2, P_3, P_2	0.5350	0.5018	0.9657	0.9899	0.9548	0.9939
Q_3, Q_2, P_3, P_1	0.5356	0.4960	0.9690	0.9890	0.9608	0.9921
Q_3, Q_2, P_2, P_1	0.4546	0.4875	0.9680	0.9918	0.9785	0.9944
Q_3, Q_1, P_3, P_2	0.5021	0.5019	0.9777	0.9941	0.9749	0.9947
Q_3, Q_1, P_3, P_1	0.4818	0.5072	0.9781	0.9939	0.9778	0.9956
Q_3, Q_1, P_2, P_1	0.5104	0.4991	0.9813	0.9932	0.9785	0.9961
Q_3, P_3, P_2, P_1	0.3990	0.5029	0.9648	0.9777	0.9561	0.9856
Q_2, Q_1, P_3, P_2	0.4566	0.5014	0.9782	0.9942	0.9748	0.9964
Q_2, Q_1, P_3, P_1	0.4742	0.5041	0.9789	0.9938	0.9774	0.9958
Q_2, Q_1, P_2, P_1	0.4481	0.4979	0.9790	0.9955	0.9786	0.9970
Q_2, P_3, P_2, P_1	0.4987	0.5149	0.9615	0.9843	0.9677	0.9919
Q_1, P_3, P_2, P_1	0.5527	0.5064	0.9765	0.9924	0.9787	0.9933
Q_3, Q_2, Q_1, P_3, P_2	0.4412	0.4995	0.9813	0.9965	0.9727	0.9981
Q_3, Q_2, Q_1, P_3, P_1	0.5446	0.5006	0.9796	0.9967	0.9743	0.9978
Q_3, Q_2, Q_1, P_2, P_1	0.5016	0.4919	0.9823	0.9955	0.9808	0.9981
Q_3, Q_2, P_3, P_2, P_1	0.4864	0.4858	0.9712	0.9910	0.9647	0.9952
Q_3, Q_1, P_3, P_2, P_1	0.5699	0.4922	0.9794	0.9944	0.9788	0.9951
Q_2, Q_1, P_3, P_2, P_1	0.4066	0.5133	0.9792	0.9947	0.9806	0.9973
$Q_3, Q_2, Q_1, P_3, P_2, P_1$	0.5370	0.4981	0.9839	0.9964	0.9792	0.9981

Table 23: The specificities achieved across the combination search by each of the six classification methods.

E AAA-L combination search results

The F_1 scores, sensitivities, and specificities achieved for AAA-L classification when employing the GB method are shown in Table 24.

Input combination	F_1	Sen.	Spec.
Q_3	0.8633	0.8561	0.8689
Q_2	0.9010	0.9103	0.8934
Q_1	0.9528	0.9630	0.9436
P_3	0.8305	0.8383	0.8250
P_2	0.8380	0.8529	0.8274
P_1	0.8005	0.7700	0.8209
Q_3, Q_2	0.9387	0.9390	0.9385
Q_3, Q_1	0.9683	0.9681	0.9685
Q_3, P_3	0.9045	0.8968	0.9109
Q_3, P_2	0.9151	0.9127	0.9172
Q_3, P_1	0.8989	0.8942	0.9028
Q_2, Q_1	0.9711	0.9741	0.9683
Q_2, P_3	0.9176	0.9256	0.9109
Q_2, P_2	0.9229	0.9328	0.9145
Q_2, P_1	0.9234	0.9258	0.9215
Q_1, P_3	0.9569	0.9558	0.9580
Q_1, P_2	0.9606	0.9645	0.9570
Q_1, P_1	0.9618	0.9609	0.9628
P_3, P_2	0.8852	0.8889	0.8824
P_3, P_1	0.8877	0.8889	0.8869
P_2, P_1	0.884	0.8858	0.8838
Q_3, Q_2, Q_1	0.9777	0.9788	0.9767
Q_3, Q_2, P_3	0.9454	0.9513	0.9402
Q_3, Q_2, P_2	0.9455	0.9498	0.9417
Q_3, Q_2, P_1	0.9481	0.9537	0.9431
Q_3, Q_1, P_3	0.9693	0.9743	0.9647
Q_3, Q_1, P_2	0.9695	0.9748	0.9647
Q_3, Q_1, P_1	0.9668	0.9642	0.9693
Q_3, P_3, P_2	0.9148	0.9105	0.9186
Q_3, P_3, P_1	0.9178	0.9232	0.9133
Q_3, P_2, P_1	0.9217	0.9163	0.9265
Q_2, Q_1, P_3	0.9770	0.9788	0.9753
Q_2, Q_1, P_2	0.9715	0.9729	0.9702
Q_2, Q_1, P_1	0.9737	0.9762	0.9714
Q_2, P_3, P_2	0.9327	0.9434	0.9234
Q_2, P_3, P_1	0.9285	0.9299	0.9273
Q_2, P_2, P_1	0.9345	0.9304	0.9381
Q_1, P_3, P_2	0.9606	0.9640	0.9575
Q_1, P_3, P_1	0.9637	0.9676	0.9601
Q_1, P_2, P_1	0.9607	0.9625	0.9592
P_3, P_2, P_1	0.8996	0.9038	0.8963
Q_3, Q_2, Q_1, P_3	0.9767	0.9781	0.9755
Q_3, Q_2, Q_1, P_2	0.9788	0.9786	0.9791
Q_3, Q_2, Q_1, P_1	0.9759	0.9791	0.9729
Q_3, Q_2, P_3, P_2	0.9484	0.9510	0.9462
Q_3, Q_2, P_3, P_1	0.9487	0.9525	0.9453
Q_3, Q_2, P_2, P_1	0.9472	0.9529	0.9421
Q_3, Q_1, P_3, P_2	0.9670	0.9654	0.9685
Q_3, Q_1, P_3, P_1	0.9673	0.9678	0.9669
Q_3, Q_1, P_2, P_1	0.9704	0.9683	0.9724
Q_3, P_3, P_2, P_1	0.9217	0.9227	0.9210
Q_2, Q_1, P_3, P_2	0.9754	0.9781	0.9729
Q_2, Q_1, P_3, P_1	0.9774	0.9784	0.9765
Q_2, Q_1, P_2, P_1	0.9772	0.9776	0.9770
Q_2, P_3, P_2, P_1	0.9352	0.9436	0.9280
Q_1, P_3, P_2, P_1	0.9587	0.9659	0.9522
Q_3, Q_2, Q_1, P_3, P_2	0.9744	0.9731	0.9758
Q_3, Q_2, Q_1, P_3, P_1	0.9820	0.9834	0.9808
Q_3, Q_2, Q_1, P_2, P_1	0.9802	0.9796	0.9808
Q_3, Q_2, P_3, P_2, P_1	0.9513	0.9541	0.9489
Q_3, Q_1, P_3, P_2, P_1	0.9725	0.9712	0.9738
Q_2, Q_1, P_3, P_2, P_1	0.9757	0.9815	0.9702
$Q_3, Q_2, Q_1, P_3, P_2, P_1$	0.9809	0.9808	0.9810

Table 24: The F_1 scores, sensitivities and specificities achieved across the combination search by the GB method.

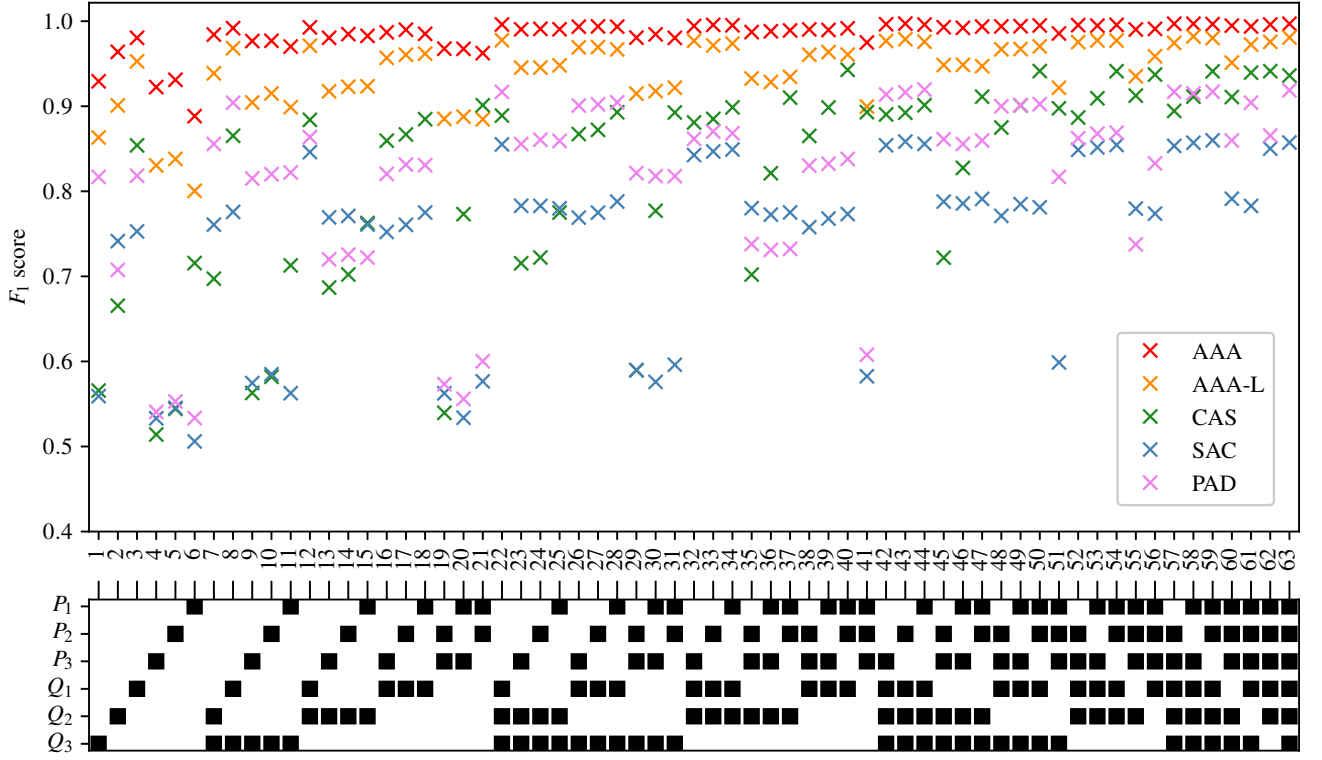


Figure 18: The F_1 scores achieved for all disease forms when employing the GB method. Measurements included within each combination are highlighted with a black square.

F GB results for all disease forms

The F_1 scores achieved for all forms of disease classification (including AAA-L) when providing each combination of input measurements are shown when employing the GB method in Figure 18.